Regional modeling of water stress

Irrigation water requirement meets water availability in the Oum er Rbia basin

Chiem van Straaten

MSc thesis
Utrecht, April 2017
Supervisors: Patricia Lopez, Geert Sterk

Cover: photos of the Tadla irrigated perimeter, taken in end November. Top left: wheat in dual-cropping with olive trees. Bottom left: a secondary channel for the distribution of water. Bottom right: field of young sugar beet crops. Top right: dug channel that diverts water from a tertiary channel to the adjacent alfalfa fields.

Student number: 5748585
MSc: Earth Surface and Water
Department: Physical Geography, Utrecht University

Contents

Abstract

Current large scale hydrological models have little value for local water resource management, even when applied regionally on downscaled data. They lack the representation of the water-transfers, allocation strategies and productivity that shape the impacts of future climate change and increased water use. This study seeks ways to improve this representation, and tests three combinations of the large scale model PCR-GLOBWB and the crop model AquaCrop, applied to a semi-arid Moroccan basin. In this region 90 percent of the water resources is required for irrigated food-production, and future scarcity is projected. The first two multi-model approaches extract water available to agriculture and express allocation to Tadla, the largest irrigated perimeter. Under historical application from 1979 to 2012, this results in a water stress index with monthly detail, and in productivity series for the dominant crops. For 2020 to 2050, RCP4.5 and RCP8.5 project an increased meteorological dryness. But only for the latter scenario does the water availability subsequently decrease, which limits crop growth severely after 2033. For the former scenario productivity increases because of CO_2fertilization. With the expressed allocation and inter-crop prioritization does this study find that production can be optimized for wheat. And that these valuable expressions for local impacts are currently lacking in the irrigation routines of large scale models. The third approach redirected AquaCrop calculations to the irrigation routine of PCR-GLOBWB to express hydrological impacts of agriculture and showed a successful application of three indicators that reflect different stages of drought.

Keywords: Agriculture, irrigation, climate change, drought, water resources, water stress.

Acknowledgements

This study is indebted to: Tarik Benabdelouahab and Abdelghani Boudhar, whose remarks gave direction to the modeling, Soundouce Moutaouakkil, for insight into MOSAICC, Riad Balaghi, for suggesting the right people to talk to, Mohammed Karrou, for his warm guidance, facilitation of my stay at ICARDA and help with collecting experimental studies, Hicham Chafqaoui, for kindly providing data and Mohamed Saaf, for facilitating my stay at ORMVAT. Supervision was in the capable hands of Geert Sterk and Patricia Lopez, with special thanks to Patricia for the modeling assistance and ever helpful comments. The Institute Agronomique et Veterinaire Hassan II is thanked for access to their research, the International Center for Agricultural Research in Dry Areas for their facilities in Rabat, the Office Regional Mise en Valuer Argicole Tadla for their facilities in Fkih Ben Saleh, and the department of Physical Geography at Utrecht University is thanked for the computational resources on their server and the fieldwork allowance.

Chapter 1

Introduction

Winter and spring are the main seasons of precipitation in the North-African region. The accumulated precipitation in these seasons is needed to sustain water use the year round, but has significantly decreased (Driouech, 2010). For the period of 1901 till 2007, this decrease was 0.5 to 1 mm per year (Schneider et al., 2011). And under anthropogenic climate change, the General Circulation Models (GCMs) point almost uniformly to a further drying of the Mediterranean (Cook et al., 2016; Stocker et al., 2013). This macroscale trend can be explained as a poleward extension of the subtropical dry zones into the North-African latitudes with a temperature increase and a precipitation decrease for all seasons (Dubrovskỳ et al., 2014).

But these measured or modeled precipitation decreases are only valid on average. Real weather in the region is subject to a high temporal variability. The historical year-to-year totals are influenced by the interannual anomalies of the North Atlantic Oscillation, that lead to recurrent periods of anomalous precipitation deficits (Driouech et al., 2009; El Jihad, 2003). Also spatial variability exists and is difficult to assess. The projections from GCMs often do not resolve the local weather processes in which the consequences of climatic change materialize (Ekström et al., 2015). Still, some of them are captured in downscaling studies for Morocco: Driouech et al. (2010) and the Modeling System for Agricultural Impacts of Climate Change - consortium (MOSAICC) (Balaghi et al., 2016), show respectively that annual average precipitation will be 5-10 percent less in 2021-2050 and 17-20 percent less in 2040-2069 (relative to 1971-2000).

However, a climate with less average precipitation does not translate 1:1 to the water resources in Morocco (Bennani et al., 2001). The exact distribution of precipitation is for instance decisive in soil moisture feedbacks, susceptibility to drought and lower discharges (Dai, 2011; Stephens et al., 2015). The nature of variability determines whether a meteorological deviation grows into one of the recurrent regional droughts (Touchan et al., 2008; El Jihad, 2003). Already since the 1980's has an increased number

of consecutive dry days led to more frequent droughts and a surface water decline (Kuper et al., 2012). But also the distribution of temperature determines (jointly with precipitation) how the snowpack in the Atlas Mountains evolves and how water resources from its melt will change (Marchane et al., 2016). Overall, the best countrywide translations of weather to water are: a reduction of annual discharge by 10 to 30 percent (Driouech, 2010) and a reduction of total surface water resources (discharge and waterbody storage) by 10 or 15 percent for the year 2020 (Bennani et al., 2001).

Simultaneously with the more frequent occurrence of droughts, water resources were further exploited. The construction of reservoirs in Moroccan basins transformed discharge into additional available water (Postel et al., 1996), and with new post-1940 irrigated perimeters, the desire for intensive food production could be met (Faysse et al., 2010). In the Oum Er Rbia basin this irrigation uses up to 90 percent of the water resources (Tahri, 2012). But not surprisingly, the exploitation reached a maximum and the fully managed basins have already been confronted with water deficits (Belghiti, 2009; Zerouali, 2009). The mismatch between availability and requirements is not merely the consequence of some interannual variability but is projected to grow structurally. Food security requires a yearly 1.6 percent increase of agricultural production and associated irrigation up to 2030 (Alexandratos et al., 2012; Elliott et al., 2014). Additional localized pressure will be exerted by a population that increasingly concentrates in urban areas (Belghiti, 2009).

The challenge of future change is therefore not solely shaped by climatic drying. As seen, the distribution of local water resources is affected physically: the nature of variability influences drought and snowmelt discharge generation, and irrigation alters the atmospheric boundary conditions (Dadson et al., 2013). But direct human influences add another layer too (WWAP, 2015): the intensely populated cities and irrigated perimeters greatly alter the availability downstream of them, reservoir operation distributes water resources over time, price effects can spawn greater demands (Lionboui et al., 2014) and technological change can lead to more efficient use (Flörke et al., 2013).

These physical, socio-economic or human-behavioral effects are not fully understood and result in large uncertainties when large scale hydrological models account for them (Vörösmarty et al., 2000b; Arnell and Lloyd-Hughes, 2014; Kiguchi et al., 2015; Zhou et al., 2015). Ideally, the Oum Er Rbia decision maker in charge of food production, could account for: (i) land use changes outside the irrigated zones that affect water accumulation, (ii) different operational strategies for the reservoirs, (iii) different irrigation strategies inside the perimeters and (iv) changes in crop productivity following the altered distribution. Because these mechanisms determine impact and adaptation. So even though large scale models promise relevant application at regional scales (Bierkens, 2015), they remain stuck at concepts

like 'natural flow' or 'renewable generated water resources' (Sperna Weiland et al., 2012; Müller Schmied et al., 2014) and have too little value for decision making in the face of regional changes (WWAP, 2015).

But model assessments have not been absent in the Moroccan water systems, as quantification already started in the 1960's (Chaponniere and Smakhtin, 2006). A first category focused on agriculture. In Balaghi et al. (2012) a combination of regression-based and dynamical crop modeling was used for seasonal forecasts, but of rainfed production only. Also the distributed and dynamical crop modeling in MOSAICC accounted for long term impacts on rainfed cereals only (Balaghi et al., 2016). A study by Gommes et al. (2008) did account for irrigated production but assumed an unlimited availability of the resource. None have been fully linked to the distribution of precipitation and surface waters. But also the second category, formed by water resources assessments themselves, did not capture the full water system. Drought monitoring is limited to meteorological indicators such as the Standardized Precipitation Index (SPI), and the operational RIBASIM model for reservoir storages needs external inflow data (Ouassou et al., 2007). One recent basin wide application of STREAM, that could capture flows everywhere, only considers the 'natural flow' and lacks the heavy human regulation (Balaghi et al., 2016).

Ideally, more model-detail is added for the mechanisms that align with the decision problems. This study therefore combines a large scale model of the basins water system with a perimeter scale model for irrigation and crop growth. First, the resulting representation of the basin's hydrological state could complement the existing SPI drought monitoring. Secondly, the link between water resources and irrigated crop productivity provides a direct metric for yield improvement under water-limitation (García-Vila and Fereres, 2012; Elliott et al., 2014). Thirdly, the setup can consider the human regulation of water to explore scenarios for water stress relief and drought management (Elame and Doukkali, 2012; Ouassou et al., 2007).

This study aims to develop and test a multi-model setup (PCR-GLOBWB and AquaCrop) for improving water resources assessment in the Moroccan Oum Er Rbia river basin. It comprises the following secondary objectives:

- Assess the water resources in the basin, expressed with drought indicators, for historical and future climate.
- Setup the crop model for water usage and production in the irrigated perimeters.
- Couple locally available water resources to the perimeters requirements, and express impacts in terms of water stress and production.
- Show an application of the setup for optimizing water use within the perimeter, under future impacts.
- Evaluate the impacts of local agricultural water use also at the operational level of the basin.

Chapter 2

Study area

2.1 Climate and hydrology

The Oum Er Rbia river is 550 km long and its basin has an area of 38,000 km^2 (Agence du Bassin Hydraulique de l'Oum Er Rbia (ABHOER), 2012). The Oum Er Rbia basin is situated between the mountain chains of the High Atlas in south-east and the Atlantic coast in the north-west (figure 2.1).

The interannual variability in precipitation is large, but also geographical variation exists. Annual precipitation varies from 1100 mm in the mountains (with on average 20 days of snowfall per year) to 200 mm in the regions close to the coast (Chaponniere and Smakhtin, 2006; Zerouali, 2009, ABHOER, 2012). The plains close to the high Atlas, where the Beni Amir and Beni Moussa irrigated perimeters are situated, recieve about 260 mm per year (Kselik et al., 2008). Over time, the Oum Er Rbia basin has been drying: Zerouali (2009) showed that average annual precipitation decreased with 2 to 8 mm per year, when comparing 1950-1970 with 1980-2000, while the available surface waters decreased by 30 percent since 1980 (ABHOER, 2010).

With its position around 32 degrees north, the potential evapotranspiration shows seasonality. In the months of July and August temperatures reach up to 50 degrees Celsius and potential evapotranspiration can be 300 mm/month. While on average, the temperature is 19 degrees Celcius and potential evapotranspiration ranges from 2300 mm/year close to the mountains to 1600 mm/year along the coast (Zerouali, 2009). This geographical difference is partly caused by landcover. The rangelands and forests in elevated regions can potentially transpire more than the croplands in the lower parts (Balaghi et al., 2012).

As a consequence of meteorological anomalies, persistent dry or wet spells occur (Dai (2011) and Appendix A). It causes the mean annual runoff in the basin to vary between 1400 and 7710 Mm^3/year. Within a period of drought, the available surface waters can decrease by 15-20 percent and rise

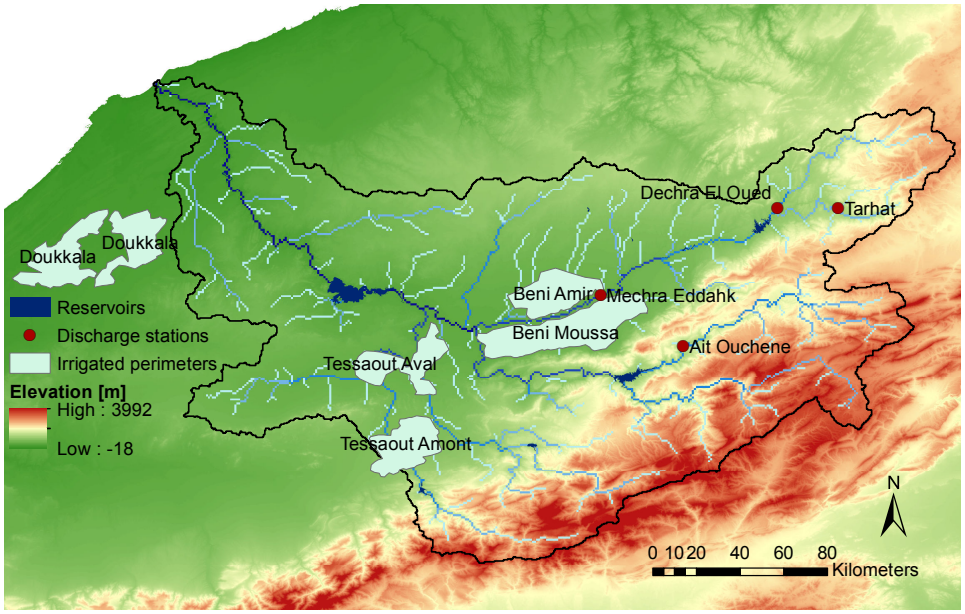

Figure 2.1: The Oum Er Rbia basin, its stream network and man-made perimeters and reservoirs. Elevation data from Jarvis et al. (2008).

again afterwards (Zerouali, 2009). The estimated long term average runoff amounts to 2511 Mm^3/year and does not flow freely. Currently, 15 reservoirs have been built in the course of the Oum Er Rbia river (the largest number in Morocco), with a total storage capacity of 5100 Mm^3 (ABHOER, 2007). But of this theoretical capacity only 3500 Mm^3 can be regulated and could potentially be available (Zerouali, 2009).

2.2 Productive water usage

A major purpose of the available water is the production of crops. Irrigation made up 90 percent of the water demand in 2008 (Tahri, 2012) and is practiced in three major perimeters that are supplied from within the basin (table 2.1, figure 2.1). One of them, the Tadla perimeter, accounts for 12 percent of the national citrus and olives production and 23 percent of the sugar beet production (Chaponniere and Smakhtin, 2006), while its parts Beni Amir and Beni Moussa occupy only 0.1 percent of the country's area.

Although there are plans for large conversion to drip irrigation (World Bank, 2016), most crops in the perimeters are irrigated with old flooding techniques, called 'robta' (Hennebert and Moerenhout, 2007; Kselik et al., 2008). The farmers separate their fields with bunds, into small plots that contain the applied water and enhance infiltration. To improve the productivity of the water percolating from the rootzones, the bunds are often planted with olive trees that can extract some it.

Table 2.1: Irrigated perimiters in Oum Er Rbia basin, after Zerouali (2009), ABHOER (2007) and World Bank (2016)

Name	Area [ha]	Demand [Mm^3/yr]	Other
Tadla - Beni Amir	28,700 - 35,000	390	Supplied by Ahmed El Hansali dam. Groundwater used for 6000 ha.
Tadla - Beni Moussa	69,500	740	Supplied by Bin el Ouidane dam. Large amounts of groundwater used. (Roerink et al., 2009)
Doukkala - Bas	61,000	550	Supplied by Al Massira dam.
Doukkala - Haut	35,000 - 64,000	554	Supplied by Al Massira dam.
Haouz - Tessaout Amont	52,000	290	Supplied by Moulay Youssef dam.
Haouz - Tessaout Aval	48,500	240	Supplied from Tessaout river and intra-basin transfers from Bin el Ouidane dam.

The food production in the perimeters is so intense that irrigation requirements can often not be met (Bekkar et al., 2007) and that availability to water's other socio-economic functions is diminished (Belghiti, 2009; Biemans et al., 2011). All users want their needs satisfied and the resources have become part of a complicated interdependence that is summarized in figure 2.2. If the estimated long term runoff is divided over the 4.5 million inhabitants of the basin, only $2511\,Mm^3yr^{-1}/\,4.5\,Mca = 558\,m^3ca^{-1}yr^{-1}$ is sustainably available. Because this is less than 600 $m^3ca^{-1}yr^{-1}$, the region classifies as suffering from water scarcity (WWAP, 2015).

Especially in the Tadla perimeter (table 2.1), the often scarce surface water is amended with groundwater pumped from one of the more than 8300 pumping wells. These are located on 47 percent of the farms (Kuper et al., 2012) and are estimated to contribute 55 percent of Tadla's total water usage (Roerink et al., 2009). For the whole basin the estimated groundwater abstraction is 622 Mm^3/yr (Zerouali, 2009), of which only 350 is deemed sustainable (ABHOER, 2007).

The resources in the basin are under additional pressure of interbasin transfers. Water is diverted to neighboring large cities like Casablanca, Safi and Marrakech to meet their industrial and domestic (drinking water) needs (figure 2.2). Additional water is transferred to the irrigated perimeter of Haouz-Central next to Marrakech (not listed in table 2.1 because of its remoteness).

2.3 Water management and institutional context

The organization that performs the transfers and operates the reservoirs is the basin agency ABHOER (table 2.2). It makes allocation decisions such

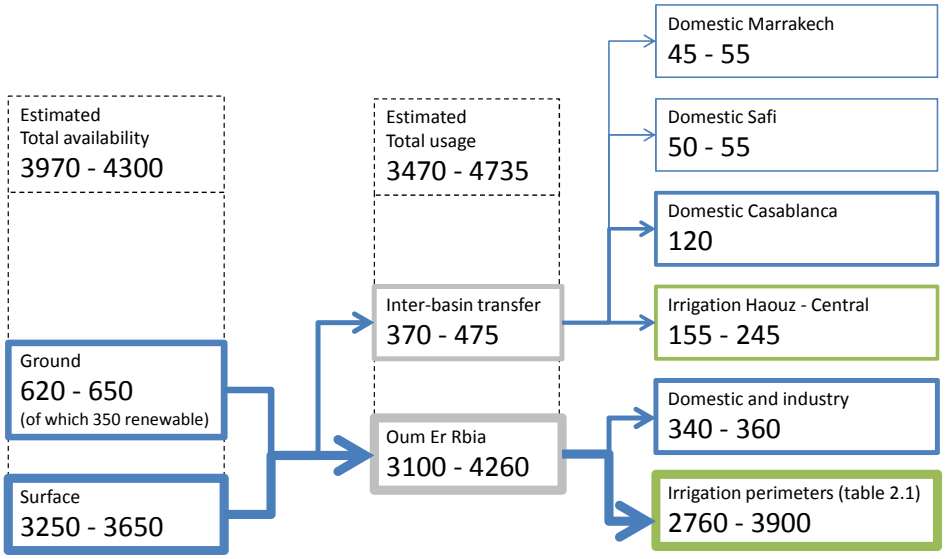

Figure 2.2: Estimates of water availability and water usage in the Oum Er Rbia basin for an average contemporary year. Water is allocated to the agricultural, domestic and industrial sectors, both within and outside the basin. All values are reported in Mm^3/yr and gathered from ABHOER (2007; 2010; 2012) and Zerouali (2009).

as: this year 100 Mm^3 is supplied to industry and 700 Mm^3 to Tadla. When the water arrives at the perimeters, distribution is taken over by one of the three ORMVA's (the Office Régional de Mise en Valeur Agricole, of Tadla, Doukkala or Haouz), who provide the water to the farmers and possibly cooperate with locally formed farmers' associations (Faysse et al., 2010).

These institutions have progressively smaller areas of control and collaborate to make water supply more adaptive to local needs. This management style has been initiated with the *Loi n. 10-95 sur l´eau* in 1995 (Doukkali, 2005) and is a response to the decrease in water resources and the population driven increase in demands, but also to the unintended effects of previous policy. After the liberalization of agriculture in 1996, cropping patterns have for instance become more water intensive (Petitguyot and Rieu, 2006). The most convincing way to deal with these continuous changes in the water system, is this new 'integrated' or 'adaptive' water resource management[1]. It means that policy is developed, implemented and evaluated in cycles (WWAP, 2015). This is done throughout the range of institutions and is

[1] *"Adaptive management accepts that irreducible uncertainties exist about future climate change, and therefore champions an approach based upon flexibility, robustness and resilience, and continuous learning. It aims at creating capacity to respond effectively to changing and uncertain conditions, using solutions that are robust under the full range of possible future climate scenarios"* (Pahl-Wostl, 2007)

Table 2.2: Institutional structure of the water sector, after Zerouali (2009) and eartH2Observe (2014).

Level	Name	Task
National	Conseil Supérieur d l'Eau et du Climat	Examines the national water plan and basin agency plans.
	Ministre de l'Energie, des Mines, de l'Eau et de l'Environnement- chargé de l'Eau (MEMEE)	Supervises basin agencies and is responsible for the planning of water resources
	Office National de l'Electricité et de l'Eau Potable (ONEP)	Responsible for drinking water provision (under MEMEE)
	Direction de la Météorologie Nationale	Data provision and research.
Basin	Basin agencies	Makes water resources plans for basin. Operates the hydraulic infrastructure. Issues rights and permits for water use. Gathers streamflow and groundwater data.
Perimeter	Offices Régionaux de Mise en Valeur Agricole (ORMVA)	Management and development of the irrigation systems. (under the ministry of agriculture)

ultimately supervised by the high council (table 2.2).

Chapter 3

Materials and Methods

3.1 Data

The Tadla perimeter has been chosen as case study. It comprises the Beni Amir and the Beni Moussa schemes and is dominated by alfalfa, wheat, maize, sugar beet, cotton, citrus and olives. The abundance of the different crops through time was reconstructed for each agricultural campaign (1^{st} of September till 31^{th} of August) in 1979-2016 (figure 3.1a). For 2012-2016 the areal values were provided by ORMVAT, but for the less recent years, a set of Tadla-studies needed to be combined. The studies that reported for specific periods (Hennebert and Moerenhout, 2007; Kuper et al., 2012; Akdim, 2014; World Bank, 2016) and those that reported for specific crop types (Addi, 2012), could be combined by assuming that from 1979 onward: (i) alfalfa and maize followed the evolution of total fodder crop in constant proportion to each other and (ii) that the amount of sugar beet, the extent of the perimeter and its overall intensity of use remained constant until the liberalization of agriculture in 1996 (Petitguyot and Rieu, 2006). These areas per crop are essential for converting the results of separate crops to total productivity and water requirement of the perimeter.

The growth of each of the crops is influenced by the soil conditions in the perimeter. Determinative hydraulic properties such as conductivity and soil water retention have previously been measured in two field experiments in the Beni Moussa scheme (Bouazzama et al., 2012; Benabdelouahab et al., 2016), and were used for this study. But to remain representative for the whole perimeter, the measured hydraulic conductivities were averaged with the values of a study in the Beni Amir scheme (Hennebert and Moerenhout, 2007). This resulted in two equally likely soil characteristics to be fed to the crop model (table 3.1).

Both the crop's water requirement inside the perimeter and the water availability given the hydrological state of the basin, are forced by weather. The forcing data in this study are precipitation, air temperature and refer-

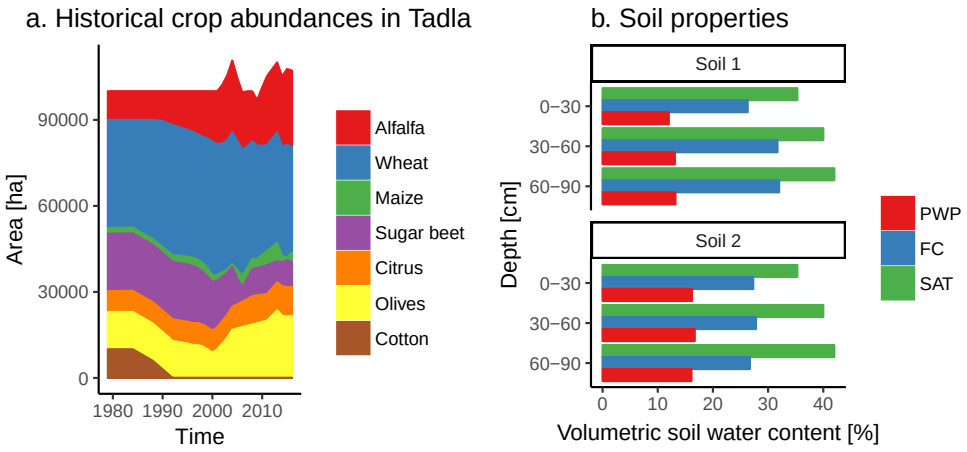

Figure 3.1: Regional input data to the AquaCrop calculations. Soil properties listed in table 3.1.

Table 3.1: Tadla soil properties used in AquaCrop, visualized in figure 3.1b.

Property (unit)	Soil 1			Soil 2		
Depth (cm)	0-30	30-60	60-90	0-30	30-60	60-90
Saturation θ_{sat} (vol %)	35.3	40.0	42.0	35.3	40.0	42.0
Field capacity θ_{fc} (vol %)	26.3	31.7	32.0	27.3	27.8	26.7
Permanent wilting point θ_{pwp} (vol %)	12.0	13.1	13.2	16.2	16.7	16.1
Hydraulic conductivity (mm day^{-1})	122	100	100	122	122	100
Sources	Benabdelouahab et al. (2015, 2016), adapted conductivity			Same as Soil 1, but field capacities and wilting points of Bouazzama et al. (2012)		

ence evapotranspiration. Historical values for precipitation were obtained from the Multi-Source Weighted-Ensemble Precipitation data (MSWEP), a bias-corrected product of merged satellite, gauge and reanalysis data, at an original spatial resolution of 0.25°x0.25° (Beck et al., 2016). Air temperature was obtained from the Watch Forcing Data methodology on ERA-Interim (WFDEI) at an original spatial resolution of 0.5°x0.5° (Weedon et al., 2014). WFDEI has bias-corrected the ERA-interim atmospheric reanalysis, while trying to preserve the continuity of large scale atmospheric systems. For reference evapotranspiration, the FAO Penman-Monteith methodology was applied: on for aspect corrected WFDEI radiation and on air temperatures corrected with lapse rates (Allen et al., 1998; Sperna Weiland et al., 2015). All three forcing variables were downscaled from their original resolution to 0.08°x0.08° (approximately 10 km at the equator). Precipitation and evapotranspiration were downscaled multiplicatively through linear regression

with the 10' CRU-CL2.0 dataset (New et al., 2002), and air temperature was downscaled by an additive correction expressed as the lapse rate times the difference between a large scale and a fine scale Digital Elevation Model (Sutanudjaja et al., 2011). For crop growth in Tadla, a clip from the basin wide sets was averaged. The period of historical analysis is 1979-2012.

The employed climate change scenarios for projecting future impacts and adaptations, were the Representative Concentration Pathways (RCP) 4.5 and 8.5 (Moss et al., 2010). The first implies a decline of greenhouse gas emissions after 2040 while in the second they grow throughout the 21^{st} century. Because the assessment of climate model uncertainties is not within the scope of this study, only the bias-corrected precipitation, air temperature and reference evapotranspiration from one GCM were used. The future values for the period of 2020-2050 were derived from the GFDL-ESM2M model runs for CMIP5 within the ISI-MIP programme (Dunne et al., 2012; Lange, 2016).

3.2 The hydrological model: PCR-GLOBWB

To assess the water availability within the basin, the hydrological model PCR-GLOBWB is used. PCR-GLOBWB is a leaky-bucket type of model that is applied on a cell-by-cell basis. It originated as a global hydrological model, coded in the PCRaster-Python scripting language (Van Beek and Bierkens, 2009; Van Beek et al., 2011; Sutanudjaja et al., 2011; Wada et al., 2014). For this study the model is used at a spatial resolution of 0.08°x0.08° and at a daily temporal resolution.

The model is forced by daily values of precipitation, air temperature and reference evapotranspiration. In this case, the leaky-buckets resemble three soil layers (0-5 cm, 5-30 cm and 30-150 cm) and one linear groundwater store (figure 3.2). Exchanges between the stores, such as capillary rise and percolation, are included and depend on the hydraulic parameters and soil moisture status of the respective layers. Precipitation is handled by an interception module and a snow module that enable the surface-storage of (melt)water. All throughfall and excess meltwater is split into infiltration and saturation overland flow, following the improved ARNO-scheme (Hagemann and Gates, 2003). The scheme gives the first soil store a gradual overflow threshold, which, in combination with percolation, explains the 'leaky-bucket' name (Bergström et al., 1995).

Potential evapotranspiration is the product of reference evapotranspiration and crop factors, and can be further lowered by soil saturation for its actual values (Allen et al., 1998). The evaporative demand is first taken as evaporation from the snow and interception storage, and then partitioned further over bare soil evaporation and transpiration.

Regarding evapotranspiration, the gridcell can be broken into: short

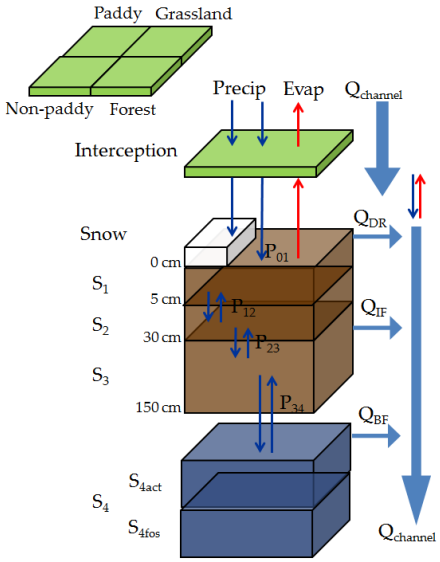

Figure 3.2: PCR-GLOBWB model structure, from López López et al. (2016). S_1, S_2 and S_3 represent storage in the first, second and third soil layer. S_4 is the linear groundwater store. Q_{DR}, Q_{IF} and Q_{BF} are the direct runoff, interflow and baseflow respectively, their summation forms the total generated runoff.

and tall vegetation, the fraction of open water and the vegetated fraction. Regarding exchange between the stores and overland flow, the subgrid variability includes: different soil types, rooting depths and surface elevations. The input data per gridcell for these land covers and soil types are given by global datasets (see Appendix B) and were not specifically gathered for this study, in contrast to the Tadla-data presented above.

The total generated runoff from a certain cell is the sum of direct runoff (saturation overland flow), interflow and baseflow. Baseflow is linearly related to the storage in the groundwater store and interflow is related to the storage in the third soil layer. This total runoff is routed in daily steps along a simplified watercourse-network of the basin (Vörösmarty et al., 2000a), that includes man-made reservoirs.

For the characteristics of the man-made reservoirs, the model usually uses the global GranD database (Lehner et al., 2011). But as multiple reservoirs were missing in the set, a new input database was constructed to increase reliability. The database was built on published statistics from AQUASTAT (FAO, 2014) and the Ministre de l'Energie, des Mines, de l'Eau et de l'Environnement- chargé de l'Eau (MEMEE, 2015). When due to the coarse spatial resolution of PCR-GLOBWB, two reservoirs were located in the same gridcell the capacities were aggregated. The total of 15 reservoirs in the basin resulted in 13 modeled ones.

The reservoir storages form part of the available resources upon which water withdrawals for (i) livestock, (ii) industry, (iii) domestic use and (iv) irrigation are imposed. The allocation rules (developed originally under global applications) dictate that demand from all sectors is met by reservoir water up to 600 km upstream and that the remainder is met by renewable groundwater S_{4act} or a nonrenewable abstraction from S_{4fos} (figure 3.2) (Wada et al., 2014).

For irrigation withdrawal, PCR-GLOBWB already posesses its own routine that models a fictional crop. The fictional crop coefficient and rooting depth are an aggregate of the multiple crops present in a gridcell and their developmental stages according to a global crop calendar (Siebert and Döll, 2010). When the extractable amount of soil moisture in the rootzone drops below a fraction of what is theoretically extractable, irrigation takes place, and soil moisture is instantaneously filled up to field capacity (Appendix B). This original routine expresses only the aggregated water usage of the fictional crop, skipping the needs and productivity of the separate crops. Although this limits its application in irrigation decision problems (because separate needs need consideration), its water balance is well connected. Some of the applied water has an evaporative influence and can drain from the rootzone, making the original routine coupled to resources on a daily basis.

The model has been calibrated with earth observation datasets available through the eartH2Observe project[1]. These are: ESA CCI Soil moisture (Liu et al., 2012) and the GLEAM evaporation product (Martens et al., 2016). The first consists of remotely sensed, passive and active soil moisture products (Kornelsen and Coulibaly, 2013), that were merged for best performance. The second dataset estimates actual evapotranspiration globally, and is based on a land surface model that assimilates remotely sensed and measured data.

PCR-GLOBWB was validated for a period of 34 years (1979-2012). It thereby included its original reproduction of the water withdrawal and regulation practices. Meaning that it accounted for livestock, industry and domestic demands in each gridcell, that irrigation was the result of the fictional grid-cell-wide crop and that water is allocated according the global rules. The resulting streamflow was compared to discharge data from four stations: Ait Ouchene, Dechra El Oued, Tarhat and Mechra Eddakh (figure 2.1), and performance was quantified with: Root Mean Square Error (RMSE), Mean Absolute Error (MAE), Nash-Shutcliffe efficiency (NSE) and Kling-Gupta efficiency (KGE).

[1] eartH2Observe is an EU (FP7 funded) collaboration that combines earth observation products and in situ datasets in multiple global hydrological models for a holistic global water resources reanalysis. This consistent integration complements meteorological reanalysis for multi-scale water resources assessments (eartH2Observe, 2015).

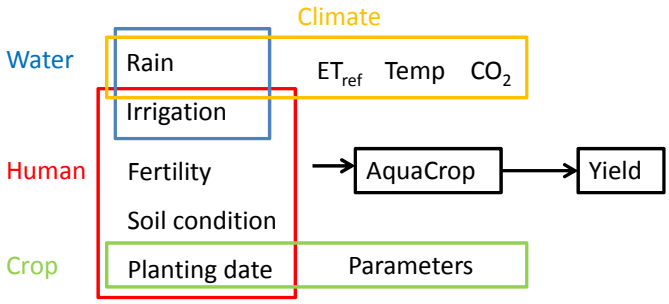

Figure 3.3: Components of AquaCrop that determine yield.

3.3 The crop model: AquaCrop

The AquaCrop model has been developed by the FAO and covers the soil-plant-atmosphere continuum of a single to multiple fields (Steduto et al., 2012). In one dimension it simulates crop development in response to water application, abiotic factors and meteorological forcing. A lot of these factors, such as the timing of irrigation and even the hydraulic characteristics of the soil are under some degree of human control (figure 3.3). AquaCrop has the ability to represent this control and can explicitly force different irrigation schedules, planting dates and fertility conditions to its physical representation of the continuum.

The climatological factor is formed by daily values of precipitation, minimum and maximum air temperature and reference evapotranspiration (Steduto et al., 2009). Additionaly, it uses annual values of CO_2 concentration for its effects on the water productivity, canopy expansion and stomatal conductance. At its core the model converts the amount of transpiration to the acquired biomass with a species dependent water productivity (mathematical formulations can be found in Appendix C). The biomass is eventually related to its harvestable portion; which is crop yield (Raes et al., 2012).

Besides biomass and yield, other characteristics of the plant: phenology, aerial canopy and rooting depth, are dynamically modeled too (Steduto et al., 2009). Although they directly influence the amount of transpiration, they are not driven by that core growth engine, but by time. Still, available water does have an influence on the parameters in these relations. Water stress effects on the crop's characterstics specifically influence its stomatal conductance, canopy expansion and canopy senescence.

Their direct influence on transpiration follows the approach of Ritchie (1972). It separates the transpiration from bare soil evaporation by multiplying either the bare soil or the crop characteristics with reference evapotranspiration (Allen et al., 1998), which is similar to PCR-GLOBWB. In the case of AquaCrop however, the dynamic crop characteristics are more than only calendar driven. And there is not just one fictional crop, but multiple,

among whom growth and water distribution differ.

To quantify the amount of stress exerted by the water content of the root zone, the model considers a balance. It keeps track of the incoming (rainfall, irrigation and capillary rise) and outgoing (runoff, evapotranspiration and deep percolation) fluxes at the boundaries of the root zone. The empirical approach to rainfall-runoff modeling is less sophisticated than in PCR-GLOBWB. But at the same time, the irrigation is not instantaneously applied to the soil profile as in PCR-GLOBWB. Instead it has a higher reality content (Nazemi and Wheater, 2015a): Just like the flooding irrigation in Tadla[2], the soil surface becomes wet and water infiltrates gradually into the profile which is discretized over twelve layers (Steduto et al., 2012).

The parameters that control productivity and the responses to stress, are different for each crop and need calibration. Hence, reported experiments from experimental sites in Tadla were collected for the dominant crops: alfalfa, wheat, maize and sugarbeet (citrus- and olive-trees could not be included in AquaCrop version 5.0). A part of the collected studies was subsequently used for validation. The dataset was formed by Sraïri et al. (2009) and Nejjam (2013) for alfalfa, Karrou et al. (2011, 2014) for wheat, Bouazzama et al. (2012) for maize, and Karrou et al. (2011) and Taky (1996) for sugar beet[3]. Wheat's parameterization was directly based on Benabdelouahab et al. (2016), who previously simulated durum wheat in Tadla with AquaCrop.

Each calibration or validation data-entry consisted of the amount of irrigation water, the planting date and the measured yield. All other factors had also to be closely approximated (figure 3.3). When not reported, the irrigation was timed according the recommendations of Karrou et al. (2011) and the characteristics of the best of the two soils were prescribed[4]. Depending on whether the experiments took place in Beni Amir (lon=-6.69, lat=32.5) or Beni Moussa (lon=-6.31, lat=32.3), location specific meteorological forcing was extracted from the downscaled data. Then, parameters were tuned to reproduce cumulative transpiration first. This made sure that water flows had the correct magnitude and thereby avoided some of the yield-equifinality from production-parameters: too little cumulative transpiration in the growth engine can be masked by a high water productivity and harvest index (Appendix C). AquaCrop-studies in similar irrigated semi-arid environments such as Alishiri et al. (2014); Ahmadi et al. (2015); Nyakudya

[2]For all historical situations only surface flooding was regarded, because nearly all localized irrigation systems have been installed for arboriculture (Bekkar et al., 2007).

[3] In cases where reported yields were fresh, a conversion to dry yields was needed. The employed dry matter contents were: $DM_{alfalfa} = 0.219$ and $DM_{maize} = 0.3331$ (Nejjam, 2013), and $DM_{sugarbeet} = 0.26$ (Choluj et al., 2004).

[4]Not regarded were the specific influences of crop species, field management, fertilization and seed quality. Because these were a factor in the experiments themselves, the model implicitly assumes the average for all these aspects.

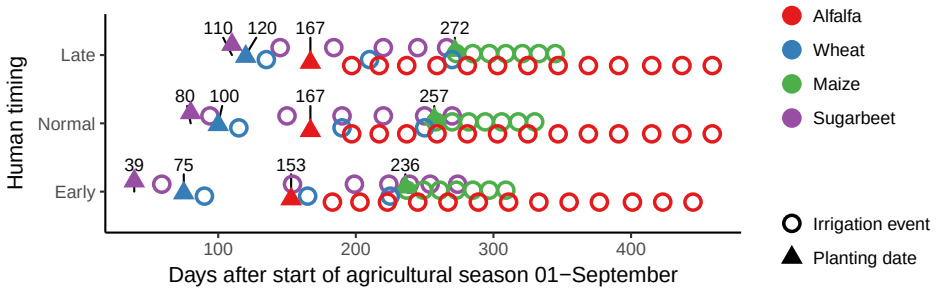

Figure 3.4: Assumed general agricultural practices for surface irrigation and crop planting. It separates human timing into an Early, a Normal and a Late scenario. Planting dates are annotated.

and Stroosnijder (2014) and the default values of Raes et al. (2012, Annex I), served as indications for the parameters, see table 3.2.

Two crop specific adjustments were made. Taky (1996) and Karrou et al. (2011) noted that premature harvesting results in a seemingly large influence of planting dates on sugar beet yields. The growing season is therefore truncated similarly in AquaCrop. Secondly, the employed version 5.0 is unable to simulate forage crops with cutting cycles. Which is why alfalfa was simulated as a 'leafy vegetable' crop, that is assumed to grow all season and is cut just before winter dormancy (Hunink and Droogers, 2011; Kim, 2015).

After the calibration and validation to data from specific experimental sites, the model needed to represent the whole perimeter and not only the specific situations. It meant that some of the large variation in Tadla (Ouzemou et al., 2015; Benabdelouahab et al., 2015) was fixed to an average field scale continuum. The 'human component' of AquaCrop was captured in three 'agricultural practice'-scenarios (figure 3.4). The irrigation and planting dates were scheduled as early, normal, or late in the agricultural campaign from September to August, and were based on the published experiments and the recommendations of Karrou et al. (2011). Together with the merged soil data (table 3.1), these fixed factors could represent the average field situation for each crop. This situation was scaled to Tadla totals with the areas for each crop and the methodologies of the next section. But beforehand the sensitivity of the model to the fixed factors was briefly analyzed.

Table 3.2: Crop parameters after calibration. Wheat completely based on Benabdelouahab et al. (2016).

		Alfalfa		Wheat	Maize		Sugar beet	
Description	Unit	Value	Comment	Value	Value	Comment	Value	Comment
Base temperature	°C	0		0	6		5	
Upper temperature	°C	30		26	30		30	
Canopy cover at 90% emergence (CC_0)	cm^2 $plant^{-1}$	1.8		1.5	6.5		4.5	(Stricevic et al., 2011)
Plant density	ha^{-1}	4e5	(Hunink and Droogers, 2011)	2.25e6	7.5e4		1e5	(Mzibra et al., 2008)
Canopy Growth Coefficient (CGC)	day^{-1}	0.215		0.05	0.153		0.082	
Maximum canopy cover (CC_{max})	-	0.87		0.94	0.96		0.98	
Canopy Decline Coefficient (CDC)	day^{-1}	0.03		0.07	0.086	Kim (2015); Ahmadi et al. (2015)	0.071	
Max rooting depth (Z_m)	m	0.9	(Karrou et al., 2011)	0.8	1		1	
Max water extraction in top of rootzone	m^3 m^{-3} day^{-1}	0.025		0.04	0.024		0.022	
Max water extraction in bot of rootzone	m^3 m^{-3} day^{-1}	0.008		0.02	0.006		0.009	
Shapefactor rootzone expansion	-	15		15	13		15	
Sowing to max rooting	day	60		103	57		60	
Sowing to emergence	day	5		12	6	(Nyakudya and Stroosnijder, 2014)	4	
Sowing to flowering	day	-		120	53	(Bouazzama et al., 2012)	110	to yield formation
Sowing to senescence	day	284		172	72		220	
Sowing to maturity	day	300		192	95	(Nejjam, 2013)	250	(Mzibra et al., 2008)
Length of flowering stage	day	-		15	12		-	
Building up of HI	day	60		48	39		140	
Maximum crop transpiration coefficient ($Kc_{tr,x}$)	-	1.05	(Steduto et al., 2012)	1.1	1.2	(Ahmadi et al., 2015)	1.15	
Normalized crop water productivity (WP^*)	g m^{-2} mm^{-1}	17.5		15	33.7		18	(Alishiri et al., 2014)
Reference Harvest Index (HI_0)	%	95		47	55		70	
Positive impact of restricted growth on HI	-	-		10	7		4	
Negative impact of restricted growth on HI	-	-		7	1	till bottom: Ahmadi et al. (2015)	1	
Depletion threshold ($p_{exp,up}$)	-	0.2	till bottom: Kim and Kaluarachchi (2015)	0.2	0.2		0.2	
Depletion threshold ($p_{exp,lo}$)	-	0.7		0.65	0.5		0.6	
Expansion shape factor (shf_{exp})	-	3		5	2.9		3	
Depletion threshold ($p_{sto,up}$)	-	0.55		0.65	0.4		0.57	
Stomatal shape factor (shf_{sto})	-	3		2.5	3		2.5	
Depletion threshold ($p_{sen,upper}$)	-	0.55		0.7	0.7		0.75	
Senescence shape factor (shf_{sen})	-	3		2.5	2.7		2.5	

3.4 Methodology

With the two models at hand, the irrigation inside Tadla could be represented either with AquaCrop: first with the average field situation per crop, and then scaled to Tadla-totals, or with PCR-GLOBWB, that represented the water requirements through a fictional crop. Because detail in irrigation and its relation to the water resources is the principal aim of the study, the original routine was replaced by AquaCrop calculations. PCR-GLOBWB was then only used to provide the water resources outside Tadla. The first two of three multi-model combinations, adress the aim to evaluate the local impacts. They express the specific impacts for Tadla in terms of water stress and production, given the basin wide water resources outside the perimeter. Approach 1 quantified the water required for sufficient production and showed how much that stresses the available resources, and an Approach 2 prescribed the available water as irrigation and quantified the resulting production. The third multi-model combination (Approach 3) evaluated regional impacts, and was used afterwards.

But before the models were combined, the realism with which PCR-GLOBWB can provide the basin wide water resources was assessed, as it should skilfully capture the regional drought propagation (El Jihad, 2003). The meteorological forcing was evaluated with common CLIMDEX indices (Alexander et al., 2006) and from the hydrological states of the represented basin indicators for different stages of drought were computed. Specifically the indicators for fast response, like soil water storage anomalies in the top 30 cm of soil and an indicator for the water limitation of evapotranspiration (Aridity Anomaly Index), but also for slower response, like the flow in the streamnetwork that is exceeded eighty percent of the time (Q80). These indicators are described in detail and with mathematical formulation in Appendix A.

Then, because inside the perimeter AquaCrop handled the irrigation, the water available for agriculture was isolated outside the perimeter from PCR-GLOBWB's spatial and temporal distribution of water resources. It meant that PCR-GLOBWB was run again with its original irrigation routine switched off, and only the withdrawals that make up the remaining 10 percent on: livestock, domestic and industrial demand. For the whole time period that the basin is then simulated, more water than usual accumulates outside the perimeter. The resulting evolution of surface water stored in the two reservoirs supplying to Tadla (Ahmed El Hansali and Bin El Ouidane) was extracted and corrected for the 240 Mm^3 that is diverted to Tessaout Aval from Bin El Ouidane (table 2.1). This way, a surface water availability for Approach 1 and 2 to local impacts, is constructed. Outside the simulation of PCR-GLOBWB, AquaCrop can then 'switch on' the irrigation of Tadla and 'use' the accumulated water resources. Similarly, the future availability was isolated for 2020-2050 under the RCP4.5 and RCP8.5 scenarios.

Table 3.3: General good yields in Tadla. The intensive values were preferably taken from surveys in the season 2012-2013, which was productive according to FAOSTAT (FAO, 2016), and were corrected to dry yields if needed (footnote 3).

	Alfalfa	Wheat	Maize	Sugar beet
Yield [t ha^{-1}]	20	5.3	12.5	15.9
Source	Nejjam (2013)	Akdim (2014)	Bouazzama et al. (2012)	Akdim (2014)

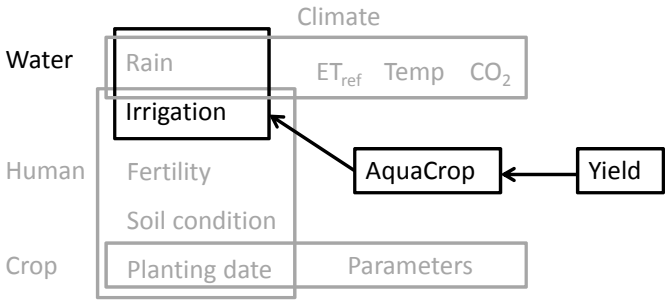

Figure 3.5: AquaCrop under Approach 1. The anticipated irrigation requirements for good yield will combine with availability of PCR-GLOBWB to Tadla water stress.

Land use, maximum reservoir capacities and other sectoral withdrawals were kept at their 2010 values.

Approach 1 couples both models after their simulations. In AquaCrop's representation of the average field it is assumed that irrigated agriculture aims for a good yield no matter the circumstances. These yield targets for the four crops were gathered from historical surveys that average out the individual behavior of farmers (table 3.3). Under the circumstances of historical or future forcing and the fixed factors, AquaCrop then iteratively computed the extra amount of irrigation required to achieve it (figure 3.5), which is of course little in rainy seasons and more in dry seasons. These intensive values (requirements on the average field for each crop) needed scaling to Tadla totals and were multiplied with the areas per crop. To remain comparable to isolated availability of surface water only, the requirements were corrected with measured crop-specific groundwater-contributions[5] (Kwelde, 2006). After an additional correction for the losses in the ORMVAT distribution network (details are presented in Appendix D) these extensive surface

[5]This is a qualitative improvement of the multi-model approach upon PCR-GLOBWB itself. On itself the general rules would have only imposed demands on groundwater when demands were not met by reservoir storage up to 600 km upstream. This practice deviates from reality in the basin and also induced a 40 percent sensitivity of withdrawals to the order of sources (Wada et al., 2014).

water requirements W [m^3] could be divided by the surface water available to Tadla A [m^3], giving a Water Stress Index for irrigation, for each month in the historical or future series:

$$WSI = \frac{W}{A} \tag{3.1}$$

But the extracted monthly reservoir storages of PCR-GLOBWB could not feed to this equation directly because two things happen simultaneously: the run's storages are only isolated in the sense that 'none is yet extracted for agriculture' while they are also subject to PCR-GLOBWB reservoir-overflow rules. This means that indeed more accumulates than usual but some of it is lost in the simulation as discharge. Following this model deficiency, only 12 months of agricultural withdrawal are accounted for, and subtracted from modeled storage to arrive at an actual storage A, making it subject to climatic variability and Tadla demands (details in Appendix D). In this first multi-model approach, the two models are combined only after their own respective simulation and come together in the final indicator.

In the second approach to local impacts, the components were combined after the simulation of PCR-GLOBWB and before the simulation of AquaCrop. Now the accumulated resources were the starting point. An actual water availability was created from the isolated resources by prescribing a monthly allocation to Tadla and accounting for the previous 12 ones. To translate this to the situation inside the perimeter, it was divided according the areas per crop and measurements of farmers' priorities (Chahri and Saouabe, 2014; Akdim, 2014) (Appendix D). These intensive amounts per crop for the average field, were timed according an agricultural practice scenario (figure 3.4). And with the circumstances of historical or future forcing, AquaCrop could calculate the impacts in actual yields of the four crops (figure 3.6).

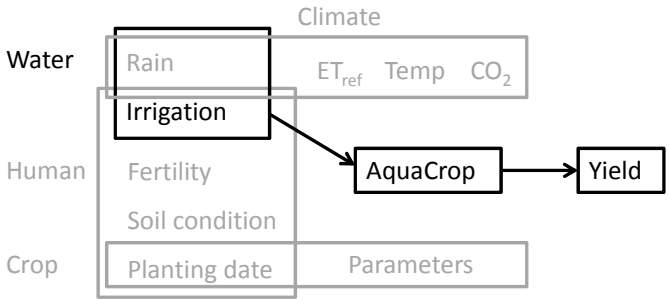

Figure 3.6: AquaCrop under Approach 2. Applied irrigation is given by PCR-GLOBWB, which in combination with other factors results in anticipated yields.

In contrast to the two local approaches above, Approach 3 made a more regional future impact assessment. Where previously PCR-GLOBWB had no irrigation in its withdrawal module (and more water than usual accumulated to be analyzed outside the model), the total Tadla requirements from Approach 1 were now supplied directly to it. These requirements for good yield under RCP4.5 and RCP8.5 then become subject to the internal global rules that distribute the water resources over irrigation and the 2010 domestic, industry and livestock demands. An entirely new simulation is formed, in which the water resources are not accumulated outside the perimeter, but where the water balance is updated for availability and withdrawals each time step. It shows the impact of change in Tadla on the basin as a whole, such as the lower availability downstream. The systemic states were indicated as previously: through soil moisture storage anomalies, evapotranspiration anomalies and discharge quantiles. During the supply of requirements, the demands for the other irrigated perimeters were assumed unaltered (values of table 2.1).

Chapter 4

Results

4.1 Calibration and Validation

4.1.1 PCR-GLOBWB

The PCR-GLOBWB version calibrated with GLEAM evapotranspiration and ESA CCI soil moisture, was initially evaluated for the time period 1979-2012 at four gauging stations: Dechra El Oued, Tarhat, Ait Ouchene and Mechra Eddahk. Streamflow estimates at these stations are shown in figure 4.1. Model discharge reproduces streamflow observations at one of the four locations well, as Mechra Eddahk shows high values of KGE and NSE (0.67 and 0.53 respectively). For two gauging stations located in the upstream part of the basin: Tarhat and Dechra El Oued, the model shows considerable bias, possibly due to the karstic nature of the soil in the north eastern region. The underground drainage in these systems may lead to a large collection of baseflow that is not simulated, causing the underestimation. Also at the station of Ait Ouchene, at an elevated position in the Atlas mountains, the discharge generating process seems imprecisely captured. Peak flows arrive earlier than observed, resulting in low efficiencies although its absolute RMSE and MAE remain comparable to the others. An indication for imprecise simulation comes also from the tributaries not covered by the discharge stations, where the simulated reservoirs of Hassan I and Sidi Driss empty momentarily.

4.1.2 AquaCrop

The AquaCrop model was calibrated and validated to experimental data gathered from previous studies at experimental sites in the Tadla irrigation perimeter. Results of the calibration for alfalfa, maize and sugarbeet are presented in figure 4.2. Wheat is lacking because previous work in Tadla already resulted in calibrated parameters for wheat (table 3.2). At first glance the calibration works well. The model-observation pairs are close to

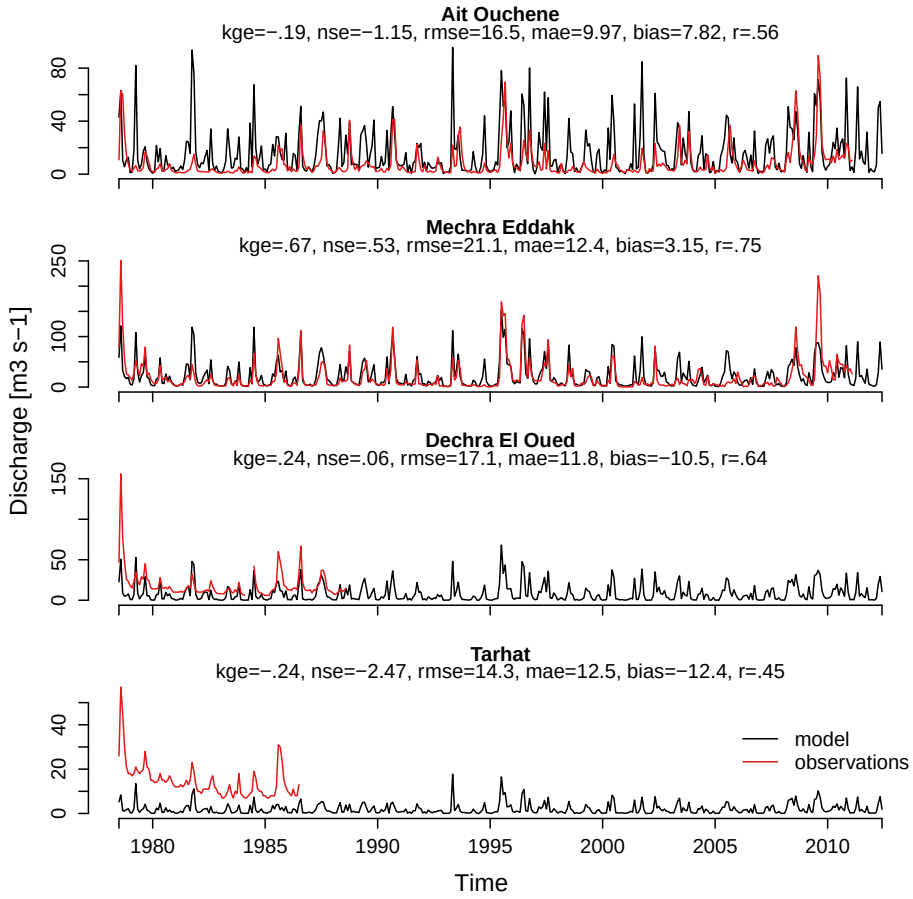

Figure 4.1: Observed (red) and modeled (black) discharge estimates at four gauging stations in the Oum Er Rbia river basin. KGE, NSE, RMSE, MAE, bias and Pearson's r are included in the panels. The unit of RMSE, MAE and bias is $m^3 s^{-1}$.

each other. For alfalfa and maize, the yields are monotonically increasing with applied irrigation, meaning that each additional application lifts some of the water limitation, both in reality and in the simulations. The purple pairs of sugar beet however, show a much greater scatter with not only a water limitation. In this case it are the different planting dates that make the yields differ by 10 t ha^{-1} for a similar application of about 300 mm. Hence, the resolved variables that additionally control the yields are growing season length and respective meteorological forcing.

The results for validation to the second half of the experimental dataset, are presented in figure 4.3. The correspondence of modeled and observed values is especially high for alfalfa, with an R^2 of 0.99. But this is partly due to its limited number of experimental observations. The green symbols of maize show an overestimation in the 300-400 mm range and an underestima-

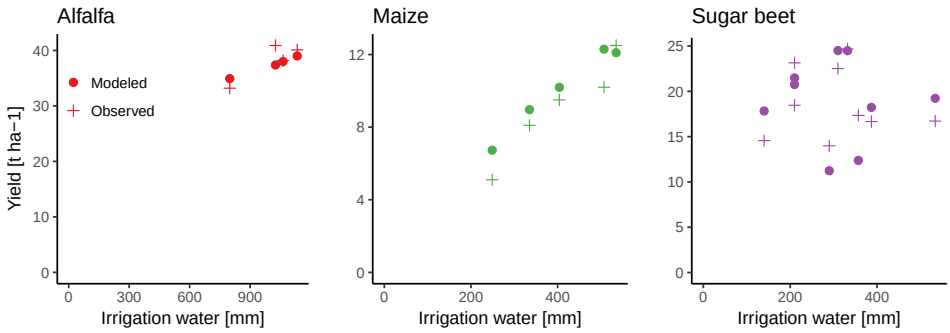

Figure 4.2: Calibration of AquaCrop to experimental studies in Tadla. The planting dates of sugar beet differ between the observation-model pairs.

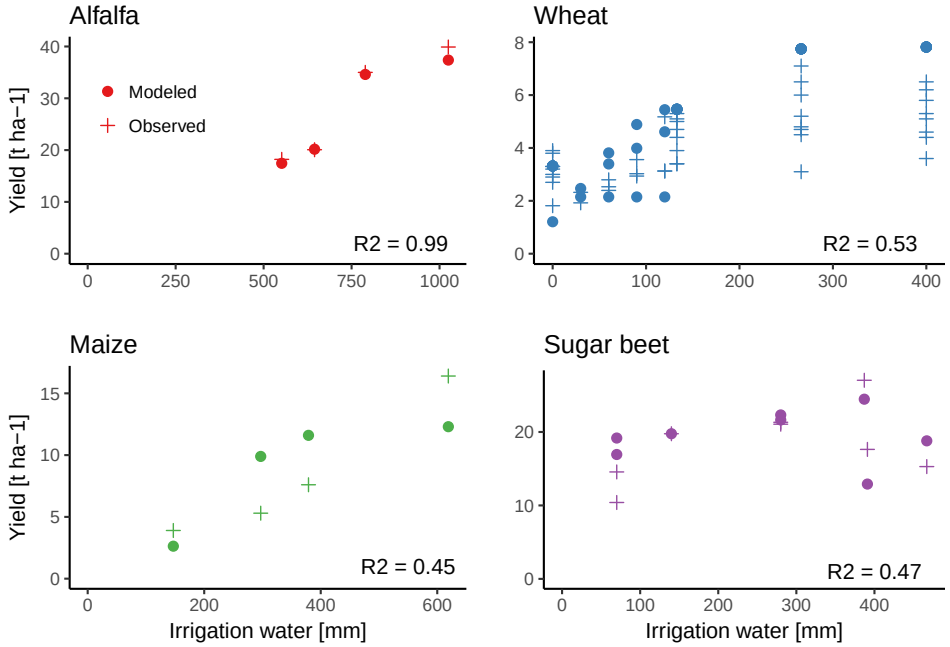

Figure 4.3: Validation of AquaCrop to experimental studies in Tadla. The planting dates of observations and reproductions differ for all crops. For wheat the observations also differ in applied fertilization and plant species. Parameter values are listed in table 3.2.

tion above 600 mm. So whereas the observed yield shows linear dependence on irrigation, the modeled relation becomes concave. The lower yield in the upper range can be explained by a real reference evapotranspiration that is higher than the modeled one (less modeled productive transpiration), or by soil characteristics that result in too much modeled water stress. Either way, the reliance on the non site-specific soil and reanalysis-based forcing results in unexplained variation. Similar unaccounted variation is encoun-

tered in the abundant wheat observations (blue, n=56). The multiple observed yields per amount of applied water deviate because the experiment included different plant species (durum and soft) and nitrogen application rates (Karrou et al., 2014). There is only a single reproduction because the model is calibrated against the average of these two factors and does not resolve them explicitly. Still, despite the inherent unexplained variance, observed values at the specific sites were both under- and overestimated. This gives confidence for the intended situations representative for whole Tadla, where variation was averaged, and where the specific irrigation schedule of the experiment was replaced with the early, normal or late timing scenario.

Figure 4.4 presents the sensitivity of the represented average field to the different fixed factors. The irrigation requirement for good yield is plotted against rainfall in the growing season of the crop under consideration. Looking at the different states of the fixed factors in the columns, it can be seen that the timing of planting date and applied irrigation influences the position of all symbols. When planted early, sugar beet (in purple, bottom left) benefits from end-of-autumn rainfall in its growing season (large values along the x-axis) and little additional water is needed. But when planted late (bottom right), these rains are missed and the model has to allocate more irrigation water to achieve good yields (lower values along the x-axis and higher values along the y-axis). Also for wheat, planting date has an influence. Because only under early planting, the rainfall is enough to require little irrigation and the crop is close to rainfed. The position of maize in the panels is very different from the other crops, but easily explained: because the growing season of maize spans only the end of spring and summer, there is hardly any rain, and irrigation requirements are high regardless of the timing.

Looking at the influence of soils it is clear that the change from Soil 1 to Soil 2 raises requirements. The extra water needed to reach the same amount of productive transpiration (yield), is especially large for wheat, maize and sugar beet. The lower transpiration per amount of water (and thus larger stresses for every amount not applied), can be traced back to the soil characteristics in figure 3.1b. Because the amount of Total Available Water (TAW = $(\theta_{FC} - \theta_{PWP}) \cdot \text{depth}$) (Allen et al., 1998) is actually lower for the second soil, the limit of full water stress ($p_{low} \cdot$ TAW, see Appendix C) is reached at less absolute depletion than in Soil 1.

When the requirements for all crops are compared to simpler crop models such as a crop factor scaling, only the values of alfalfa and wheat seem to deviate. The studies of Hennebert and Moerenhout (2007) and Akdim (2014) found respectively that irrigation of alfalfa amounts to 1000 or 1400, wheat to 320-570, maize to 230-700, and sugar beet to 630-780 mm. Still, the crop factor scaling is only a crop specific adaptation of the reference evapotranspiration ($ET_{c,act} = ET_{c,pot} = k_c \cdot ET_{ref}$) and assumes therefore a full meeting of the evaporative potential. Whereas in reality, and in the

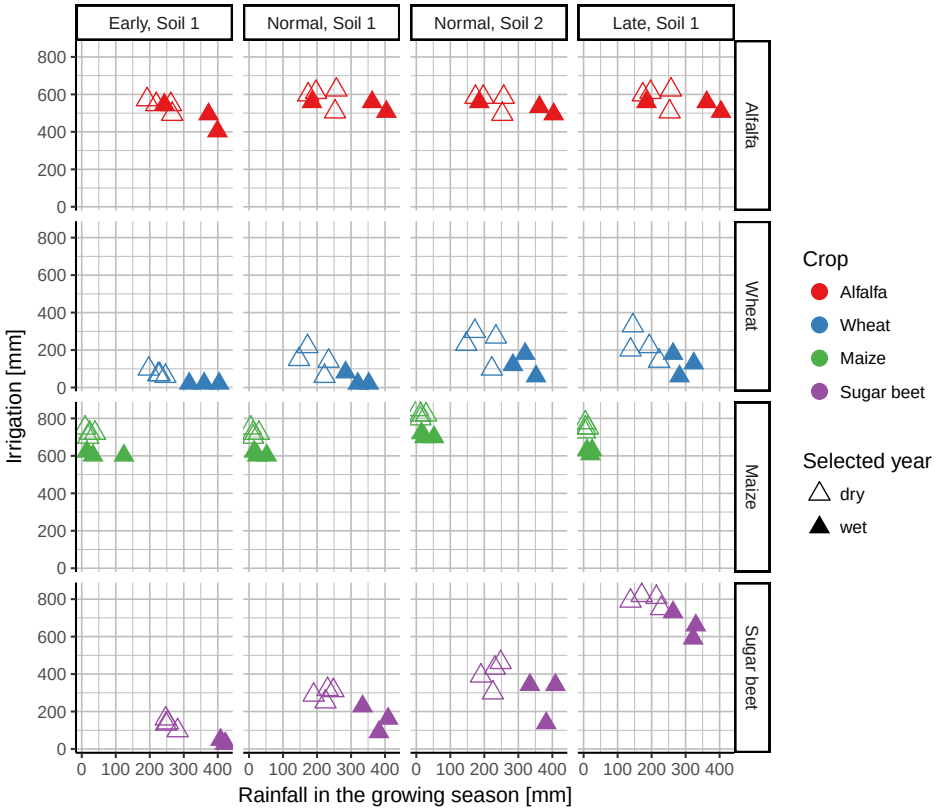

Figure 4.4: Sensitivity of intensive irrigation required for good yields on the average field in Tadla. Plotted for wet years and dry years, and for Soil 1 in combination with early/normal/late timing and Soil 2 with normal timing. Wet campaign selection: 1990-91, 2008-09, 2010-11 (Ouraich et al., 2014). Dry campaign selection: 1982-83, 1994-95, 1999-00, 2007-09 (Doukkali, 2005; Balaghi et al., 2012; Ouraich et al., 2014; Ouassou et al., 2007).

present AquaCrop simulations, the irrigation remains sub-optimal through water limitation (Benabdelouahab et al., 2015).

The influence of water limitation in the panels is best visible as the differences between dry and wet agricultural campaigns. It rains less in the dry years no matter the human timing. Subsequently, a lowered rainfall leads to higher requirements for all crops. For the time series of the following multi-model approaches, year to year variations can thus be expected. To structure their presentation, only the results for Soil 1 and normal planting are plotted, but relative behavior remains as explained here.

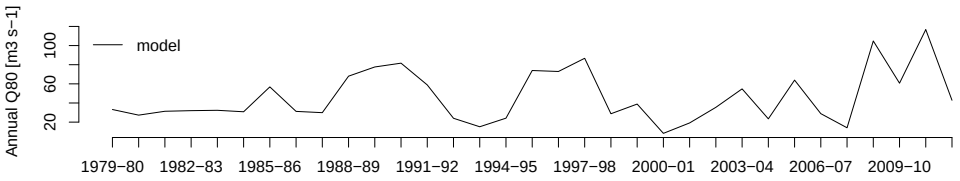

Figure 4.5: Modeled hydrological dryness (Q80) at the basins outlet per agricultural campaign.

4.2 Multi-model: Historical analysis

The sensitivity analysis showed that precipitation induces variability in the requirement simulations in Tadla. But also the distribution of water resources in PCR-GLOBWB is influenced by it. A skillful MSWEP precipitation product, with respect to the regional regime of recurrent droughts is therefore needed (El Jihad, 2003). With a threshold of 1 mm to categorize the basin-average rainfall as a wet-day event, an analysis of CLIMDEX indices was made for the winter spring rainy season from 1979 to 2012. It showed that each period of January to April is likely to have only 32 wet days and a maximum of 25.5 consecutive dry days (see also table 4.2). Hence the desired (reliability wise) dry spells are present.

Hydrologically, the system is affected by the meteorological anomalies. An anomalous low amount of precipitation or enhanced evaporation (through temperature, relative-humidity, wind or radiation) can propagate through the basin's system (Dai, 2011). The realism of PCR-GLOBWB to simulate this was assessed with the different drought indicators.

At a low temporal resolution and with the slow-response indicator for low-flow (Q80) at the outlet, the evolution of drought is presented in figure 4.5. It shows that the historical reproduction of PCR-GLOBWB coincides with known basin-wide hydrological droughts: the index indeed reaches its lower values for the dry agricultural seasons: 1980-81 and 1994-95 (Ouassou et al., 2007), 2000-01 (Ouraich et al., 2014) and 2007-08 (ABHOER, 2010).

These annual scale droughts grow from anomalies with a higher temporal resolution, and a realistic representation of these is desired for a model that updates its water balance daily. In figure 4.6 similar timeseries are presented as in figure 4.5, but now with all three indicators. The time axis is omitted and their temporal behavior is summarized with the number of months that significant auto-correlation is displayed (Box et al., 2015). In the left panel the soil moisture anomalies show the lowest temporal auto-correlation. Although this buffer in the top 30 cm of soil is affected first, it provides only a weak and, as seen from the inter-quartile range, relatively symmetric feedback. So commonly the anomaly is dampened after 3 months by renewed variability. But a longer temporal persistence of 4 to 5 months is found for the soil moisture status in the entire rootzone, as indicated by

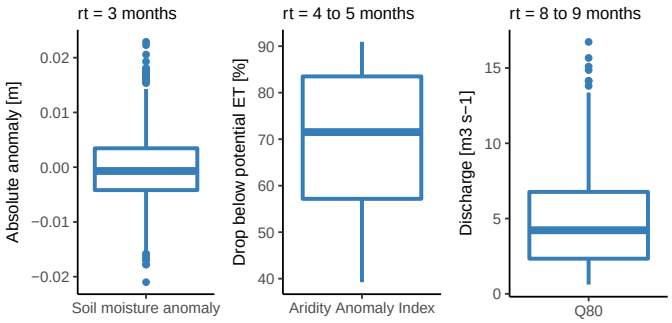

Figure 4.6: Boxplots of monthly drought indices from 1979-2012. The months of significant temporal auto-correlation rt ($\alpha = 0.05$) are included in the title. All indices are spatially averaged for the basin. Soil moisture anomaly is computed for the top 30 cm.

the Aridity Anomaly Index (a measure for how water limited the potential evapotranspiration is). The strong lowering of atmospheric moisture by a drop in transpiration is the cause of a stronger feedback, seen in the negative skew of the distribution. In the right panel, the low flow (Q_{80}) in the streamnetwork is presented. When an anomaly has propagated through the soil moisture stores, and baseflow from the fourth groundwater store becomes less, the temporal auto-correlation is larger as it takes longer for a wet spell to re-equilibrate with drainage and capillary rise. Because the simulations of PCR-GLOBWB appear to give a realistic drought regime, it is clear that these indicators can complement the existing drought monitoring which is only limited to the SPI.

Inside the perimeter, the irrigation routine of PCR-GLOBWB itself es-

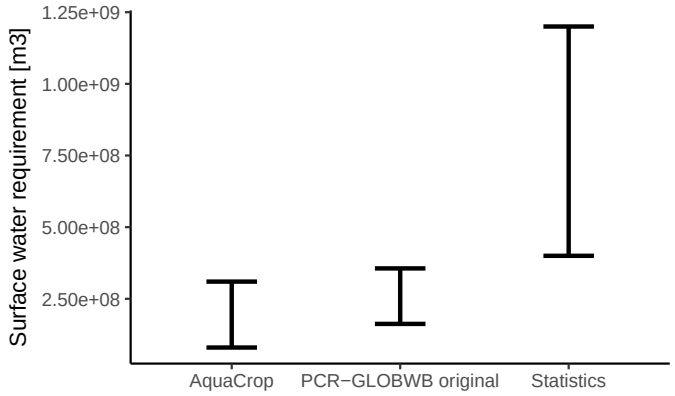

Figure 4.7: Historical irrigation requirements of surface water, per agricultural campaign for the whole of Tadla in 1979-2012. The AquaCrop requirements are computed with Approach 1. The comparison is made to ORMVAT statistics of the actual surface water allocation.

timates the Tadla surface water requirements from 1979 to 2012 to vary around 2.5e8 m^3 (figure 4.7). Compared to the actual reported surface water allocation to the Tadla scheme (provided by ORMVAT) this is an underestimation. This routine was replaced by the calculations of AquaCrop, which in Approach 1 and 2 is done outside the simulation of PCR-GLOBWB. Depicted in the figure is that the total good yield requirements of Approach 1 are similar in magnitude to the PCR-GLOBWB routine, but show a slightly larger range as the minimums are lower.The previous finding in the sensitivity analysis that requirements per crop are higher in dry years and lower in wet years, thus also applies to the totals. But the range shown in the statistics is much larger: 4e8 to 1.2e9 m^3. The reasons that Approach 1 in the figure underestimates the total surface water allocation can be sought in its representation of the average field for the four crops, or in the upscaling procedure. In case of the latter, the area per crop, the groundwater corrections and the distribution efficiency, could incorrectly scale the represented soil-plant-atmosphere continuum. But in case of the former, the on-field water use efficiency may be too high.

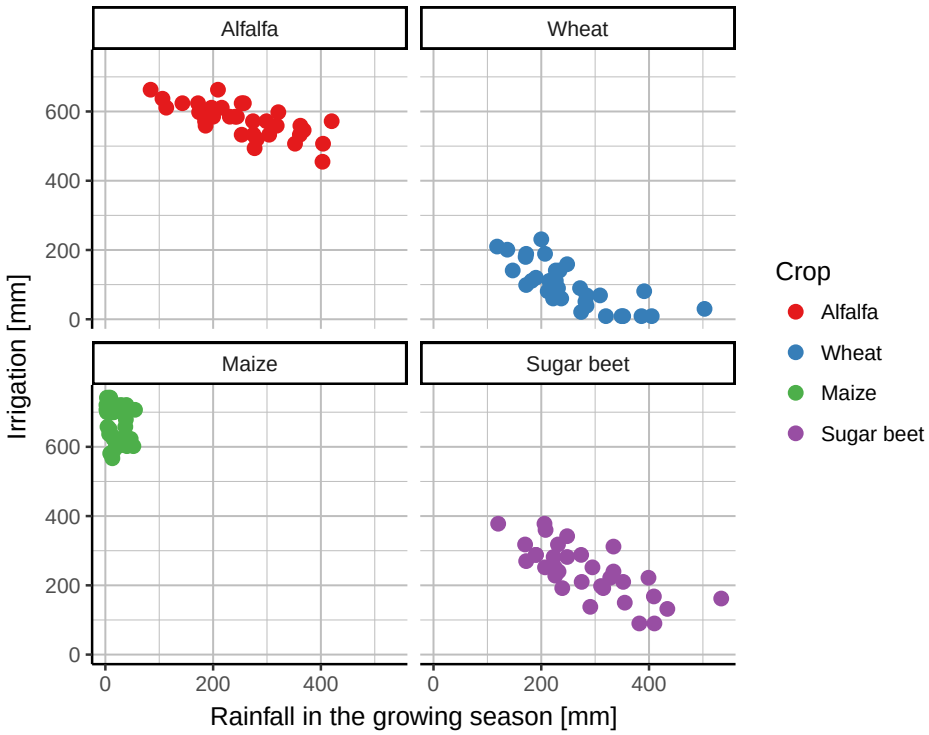

Figure 4.8: Water requirements for good yield. One dot for each agricultural campaign in 1979-2012. The intensive values per crop are calculated with Approach 1 to AquaCrop. Rainfall differs per crop due to the timing of their growing seasons.

The per field situation given Soil 1 and normal timing is presented in figure 4.8. The crops are placed in rainfall versus irrigation panels, similar to the sensitivity analysis. As each point represents a single agricultural campaign, the year to year variation is visible. The position of maize is again determined by its spring-summer growing season. Striking for wheat is the ability to be rainfed at 300 plus mm of rainfall (which occurs akin the real growth of many cereals in the rainfed zones (Balaghi et al., 2012)). Sugar beet also shows a decreasing requirement with increasing rainfall. For alfalfa this effect (negative slope) is less pronounced. Its requirements remain high in wet years.

After scaling of the separately calculated AquaCrop requirements for good yield, Approach 1 combined these perimeter totals with the (more than usually) accumulated reservoir storage outside the perimeter, extracted from PCR-GLOBWB. Meaning that the models were are combined only in the metric of the Water Stress Index, after their respective simulations. In figure 4.9 (right panel) this first expression of local impacts can be seen. The requirements were subtracted within the moving window to arrive at actual reservoir storage (purple line). As the modeled requirements were an underestimation, the actual storage and thus the denominator in the index remain high (previous withdrawals have little impact). WSI (green line) is therefore low. The model performs badly in this sense because the index is further lowered by the underestimated requirements themselves in the numerator. Despite the magnitude mismatch, it is visible that for two decades (1980-2000) the storage decreases as one expects from the reported drying (ABHOER, 2010). However the availability rises artificially after the Ahmed

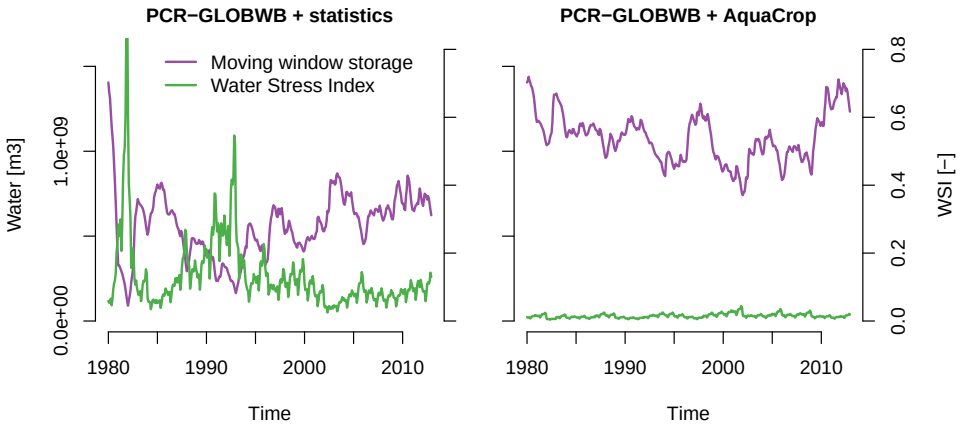

Figure 4.9: Approach 1. Historical multi-model combination of PCR-GLOBWB surface water availability to Tadla, reported annual statistics by ORMVAT (projected to months, see Appendix D) and AquaCrop requirements. Together they result in actual storage (left axis) and the Water Stress Index for local impact (right axis).

El Hansali dam was constructed in 2001, meaning that former discharge is now counted as reservoir storage. While in reality the availability decreased further and the construction had only a marginal influence on the total[1] (Belghiti, 2009).

To assess what kind of water stresses the fully modeled setup ideally should capture, the whole is compared to a similar combination of PCR-GLOBWB storage with the historical statistics, after these were projected to months (Appendix D). Periods of low storage (for example 1994) raise the magnitude of the demands relative to the availability, giving spikes in the WSI (left panel, green line). Computed over the whole time span, the behavior leads to a Dynamic Water Stress Index of 0.3, which accounts for the frequency and duration aspects of water stress (Appendix A).

In Approach 2, AquaCrop and PCR-GLOBWB were again used to express local impacts, but now in terms of yield. The combination was made after the simulation of PCR-GLOBWB and before the simulation of AquaCrop. The outside the perimeter accumulated water resources of PCR-GLOBWB were converted to an actual availability by prescribing a set of releases. These annual surface water releases for each agricultural campaign range from 6.3e8 to 8.7e8 m^3. Although the minimums are higher and the maximums lower than the actual statistics presented previously, do these releases correspond much better than the requirements of Approach 1 (figure 4.7).

With this relatively narrow range of releases it needs a description of how water is divided over all locations inside the perimeter and how that translates to the AquaCrop representation of the average field. It is therefore divided according the historical cropping patterns, groundwater contributions and prioritizations by farmers (Appendix D). After downscaling the ranges of modeled applied intensive water remain narrow (table 4.1), but are high. Which is the result of either the scaling procedure or a large accumulation in PCR-GLOBWB. Alfalfa receives the most, as it is also the most water consuming crop in reality (Akdim, 2014). Wheat is allocated more than on general required for good yield in Approach 1, while sugar beet and maize recieve amounts similar to the earlier ones (figure 4.8).

[1] It is unclear in most sources what counts as a surface water resource. When the reported totals includes both storage and discharge, then the artificial rise in the model happens only because surface water resources are defined as reservoir storage only.

Table 4.1: Approach 2. Ranges of 1979-2012 intensive total irrigation [mm yr^{-1}] to Tadla, given the releases from water availability accumulated in PCR-GLOBWB and treated with a downscaling by cropping patterns, measured groundwater contributions and inter-crop prioritization.

Alfalfa	Wheat	Maize	Sugar beet
2000-1500	580-420	900-700	330-250

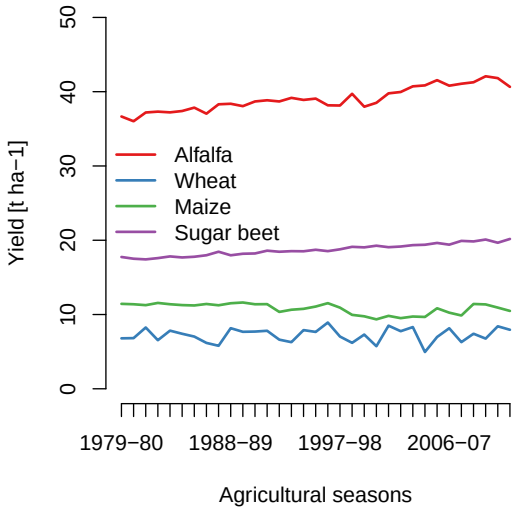

Figure 4.10: Approach 2. Intensive yields from 1979-2012 were derived from intensive surface water prescribed to AquaCrop (table 4.1).

When AquaCrop is forced with these intensive amounts of irrigation, timed according the normal scenario, and with historical weather series, it results in the yields of figure 4.10. The increasing yields for alfalfa and sugar beet follow from the high amounts of applied water. There is so much of it that canopy expansion- and stomatal closure-stress hardly occur. The maximum amount of transpiration is often reached, and the slight heightening of normalized water productivity (biomass per unit transpiration) by CO_2 enlarges their yield over time. For maize this effect is not visible due to the more pronounced water limitations. Wheat shows the most variation, especially since its number of irrigation events is only three in the simulation (see figure 3.4), and also small in reality. A dry spell in an un-irrigated period can therefore limit leaf expansion during the crop establishment. But interesting enough, wheat yields are larger than the 'good yield' of Approach 1, which indicates that either AquaCrop underestimates the water stress or that the good yield value is chosen to low[2].

4.3 Multi-model: Future analysis

From climate projections the dryness of the region is expected to increase. To test whether this meteorological effect is present in the forcing data, several CLIMDEX indices for the future precipitation were calculated. They are presented in table 4.2. Both the RCP4.5 and RCP8.5 rainfall distributions

[2]Whether taken from surveys or modeled in Approach 2, average yields remain difficult to validate. The reports are dispersed and hindered by the difficult to capture spatial variation (Ouzemou et al., 2015).

Table 4.2: Historical and future Oum Er Rbia precipitation. The values (val) of several CLIMDEX indices (Alexander et al., 2006) were calculated for winter/early-spring (jan-april) and over the whole basin, with an assumed wet-day-threshold of 1 mm. The presented relative change (rel) is between the historical (MSWEP) and the RCP4.5 and RCP8.5 precipitation forcing (GFDL-ESM2M). Comparison is made to changes found by Driouech et al. (2010) for the whole of Morocco in the SRES-A1B scenario using ARPEGE-climate.

	MSWEP	RCP4.5		RCP8.5		(Driouech et al., 2010)
Index	val	val	rel [%]	val	rel [%]	rel
Mean precipitation [mm]	1.5	1.5	-0.6	1.2	-19.6	-15 %
Nr. of wet days	32.2	20.3	-37.0	18.3	-43.1	- 10 to 25 %
Nr. of max. consecutive dry days	25.5	34.9	37.2	36.1	41.6	+ 4 days
90^{th} percentile of wet day rainfall [mm]	10.8	15.9	47.3	15.1	39.1	none found

in 2020-2050 seem to differ substantially from the historical one. Periods of more intense dryness can be expected as progressively for RCP4.5 and RCP8.5, the number of wet days decreases and the number of consecutive dry days increases. Although the number of wet days decreases, the one that do occur show extremer amounts of rainfall that generally have a higher proportion of runoff. In both scenarios this positive increase of the 90th percentile rainfall is found. This is not only caused by the specific choice of products (MSWEP and GFDL-ESM2M) because most changes agree with the values of Driouech et al. (2010) in the last column. As established in previous chapters the precipitation distribution is not easily translated to its effects on regional water resources and crop growth inside the perimeter. The exact effects are determined in combination with the other variables as temperature and reference evapotranspiration.

Overall, when AquaCrop was switched on as the perimeters module for irrigation, it gave surprising results in Approach 1. The Tadla totals after scaling the average field situation per crop, are presented in figure 4.11. Compared to the historical simulation the ranges in both scenarios are narrower. And compared to the reported historical statistics the estimations seem to suffer from underestimation again. They are the result of a scaling that assumed that the 2015-2016 cropping pattern and historical groundwater contributions were still applicable (it implies a rigid agricultural sector that does not adapt). The difference with the historical AquaCrop range thus needs to be sought on the field itself.

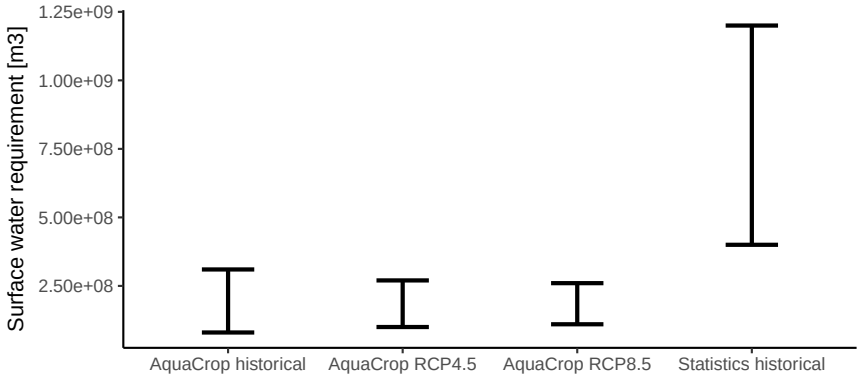

Figure 4.11: Future surface water requirements per agricultural season for the whole of Tadla in 2020-2050. The AquaCrop requirements are computed with Approach 1. Surface water allocation statistics supplied by ORMVAT and the historical AquaCrop assessments for comparison.

The situation for the average field is presented in figure 4.12 with the requirements for a good yield. For the thirty agricultural campaigns in 2020-2050, the shift towards drier conditions means that the rainfall in the growing seasons will be less, while temperatures and atmospheric CO_2 contents rise. Relative to the historical situation (figure 4.8), the maximum requirements of all crops, except maize, drop a little. This is counter-intuitive because the minimum rainfall becomes less, most notably for sugar beet and wheat, for whom 50 mm rainfall is non-existent in the historical period. Also between the scenarios RCP4.5 (left) and RCP8.5 (right) the rainfall distributions differ, as median rainfall is less in the latter. In both comparisons the lack of a clear subsequent increase in requirements is partly caused by more productive transpiration under heightened CO_2-contents (Steduto et al., 2012). For maize, especially under RCP8.5, the relationship is also influenced by secondary temperature stresses on flowering. Like previously, wheat grows almost without irrigation whenever the rainfall amounts to 250+ mm. But this occurs less in RCP8.5 and narrows its minimum requirements, which in combination with the drop in maxima, is magnified by the areas per crop and seen back in the narrower totals (figure 4.11).

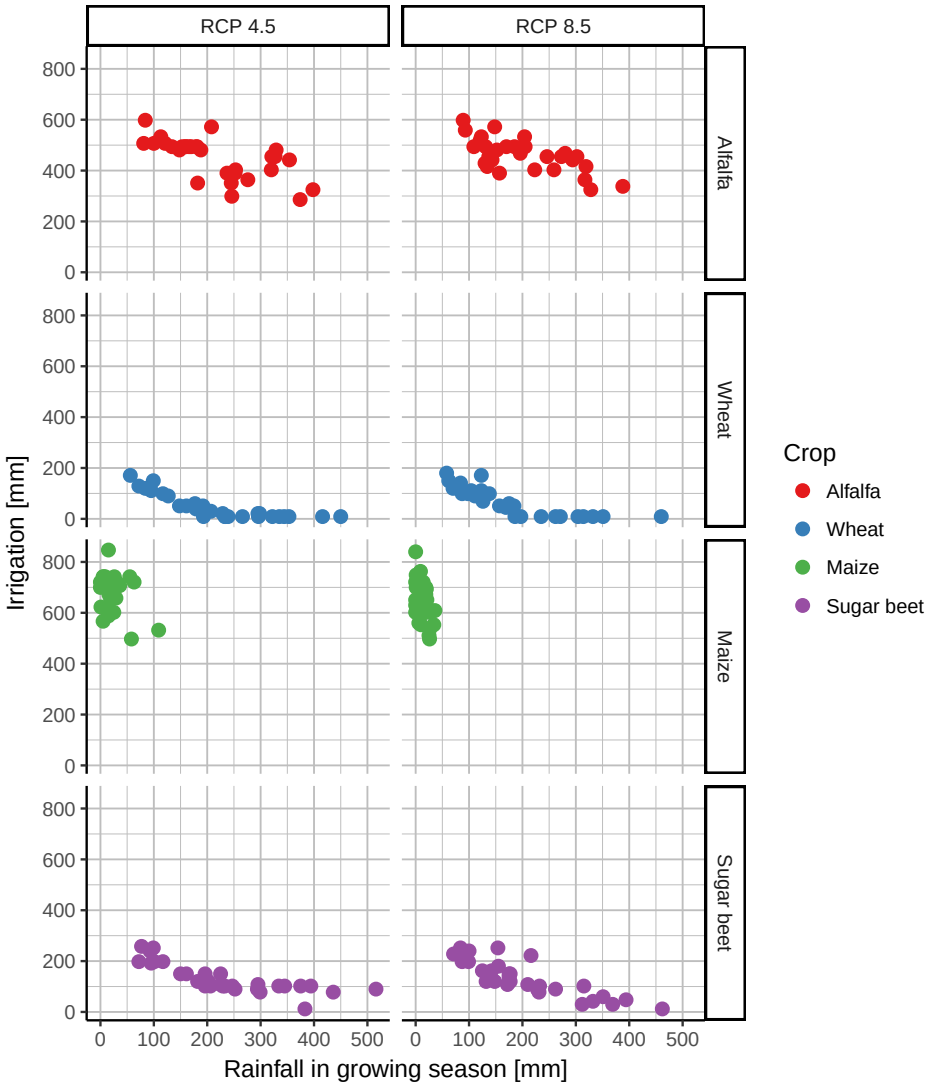

Figure 4.12: Irrigation water requirements for good yields in RCP4.5 (left) and RCP8.5 (right). One dot for each agricultural campaign in 2020-2050. The intensive values per crop are calculated with Approach 1 to AquaCrop. Rainfall differs per crop due to the timing of their growing seasons.

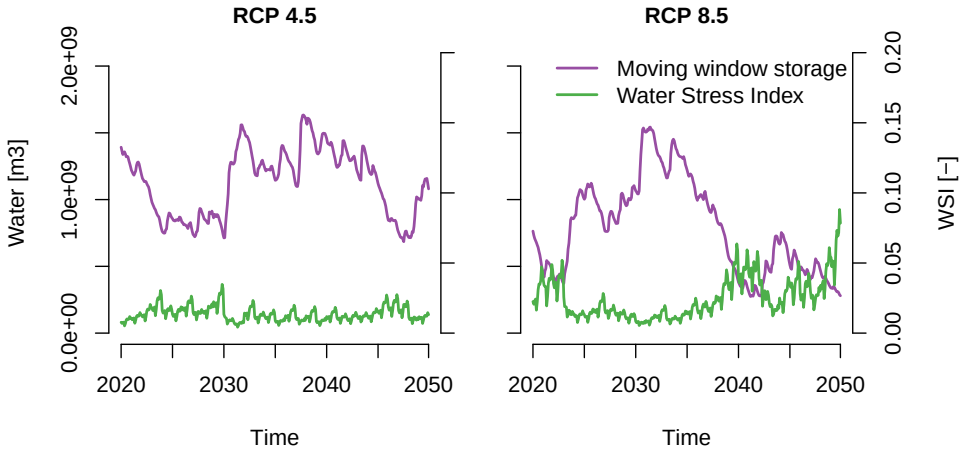

Figure 4.13: Approach 1. Future multi-model combination of PCR-GLOBWB surface water availability to Tadla and AquaCrop requirements. Together they result in actual storage (left axis) and the Water Stress Index for agriculture (right axis).

When in Approach 1, after both their simulations, the totals were combined with PCR-GLOBWB water availability accumulated outside Tadla, the underestimation was once again passed on to the local WSI impacts. But through its denominator the WSI is also influenced by water availability in PCR-GLOBWB, which we expect to decrease under the percieved drying in the precipitation distributions. And indeed, the increased dryness is reflected in the actual storages as accumulated in PCR-GLOBWB and corrected in the moving window. The actual storages in figure 4.13 drop to lower values than those in the fully modeled historical series (figure 4.9, right panel): 4.4e8 as opposed to 7.5e8 m^3. The actual storage in RCP8.5 is on average lower than in RCP4.5 and also drops sharply after 2033. Regardless of the underestimated requirements that are passed on, this hydrological drying results in a trend of increasing water stress, which is especially peaked in summer months[3].

In Approach 2 the models were combined after the simulation of PCR-GLOBWB but before the simulation of AquaCrop. It also expressed local future impacts, but not in terms of Tadla totals, but in terms of average on-field yields. The accumulated water of PCR-GLOBWB and its corresponding releases are already impacted by the climate change effects in the simulation and range from 5.0e8 to 9.9e8 m^3 in RCP4.5. They remain comparable to releases of the historical Approach 2 and likewise also much more comparable to allocation statistics (4e8 to 1.2e9) than Approach 1 (figure 4.11). However, for RCP8.5 the overall distribution shifts and the minimum

[3]The summer peaks agree with the fact that annual water stress quantifications can conceal the short-lived impacts that are experienced in reality (Brauman et al., 2016; Mekonnen and Hoekstra, 2016).

Table 4.3: Approach 2. Ranges of intensive irrigation [mm yr^{-1}] to Tadla under climate change, given the 2015-2016 cropping pattern, measured groundwater contributions and inter-crop prioritization.

	Alfalfa	Wheat	Maize	Sugar beet
RCP 4.5	2000-1000	600-330	900-500	330-180
RCP 8.5	1800-500	560-170	830-250	300-90

annual allocation of 2.6e8 m^3 forms an unprecedented low.

To make the translation to the situation on the average field, the releases were converted with the rigid agriculture assumption, divided with the cropping patterns, prioritized according the agricultural practice and corrected for groundwater contribution. The resulting amounts of intensive irrigation remain high (table 4.3), especially for alfalfa, just like the historical situation. They however range substantially from year to year. The unprecedented low allocations to alfalfa, wheat and maize, following from the low releases under RCP8.5, are even halve of the historical minimums (table 4.1).

On the basis of these, AquaCrop simulated an absence of water limitation for alfalfa and sugar beet for nearly all periods in RCP4.5, which through the enhanced water productivity by CO_2, results in slightly rising yields (figure 4.14, left panel). Wheat however, experiences water stress and stomatal closure, which for maize adds to the known temperature stresses and failure of pollination. In RCP8.5 (right panel), the low allocations from 2033 onward start to limit the yields of wheat and maize (blue and green line). When intensive application to alfalfa hits the lower values around 500 mm about a decade later, AquaCrop simulates a decrease of alfalfa yields too.

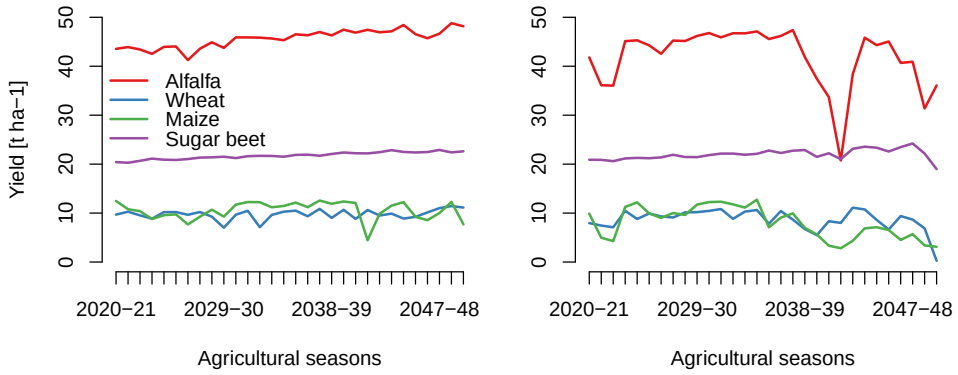

Figure 4.14: Approach 2. Projected yields when AquaCrop is forced with water availability for RCP4.5 (left) and RCP8.5 (right) in table 4.3.

Besides quantifying impacts in an un-adapted agriculture, a decision maker is ideally able to calculate the effects of adaptation too. The Approach 2 setup therefore tests an adaptation strategy, with a new expression of 'how agriculture in Tadla works' to scale the same accumulated availability of PCR-GLOBWB. The strategy is an adaptation to the effects just described; that from time to time wheat is likely to become water limited and sugar beet hardly so. Hence, the parametric key was adapted to allocate more to wheat and maize, and less to sugar beet. This led to new irrigation applications per crop on the average field. And over the whole period of 2020-2050 under RCP4.5 it altered the extensive production totals by -4.7e5, +3.6e5, +7.3e4 and -1e3 tonnes for alfalfa, wheat, maize and sugar beet respectively. So while alfalfa decreases, this is compensated by an increase of wheat that is only 1.1e5 tonnes less. Which is a good result if one values wheat more than alfalfa. It reveals that this local adaptation in the form of optimizing the biophysical production of crops, can even be explored economically, when coupled to valorization.

The previous multi-model approaches have quantified the impacts as water stress in Tadla or as the yields on the average field. They have in common that it are local impacts. The regional assessment of Approach 3 still replaces the original irrigation module of PCR-GLOBWB with the calculations by AquaCrop. But in this case it is not outside the water resources simulation, but internally. It feeds the irrigation requirements for good yield (after simulation in AquaCrop Approach 1) directly to the withdrawal module of PCR-GLOBWB. The resulting simulations are not fully dynamic (it lacks the return flow of percolated water from the AquaCrop soil profile to the groundwater reservoir (Kselik et al., 2008)) but water resources are consistently updated for all withdrawals. But because the updating happens by

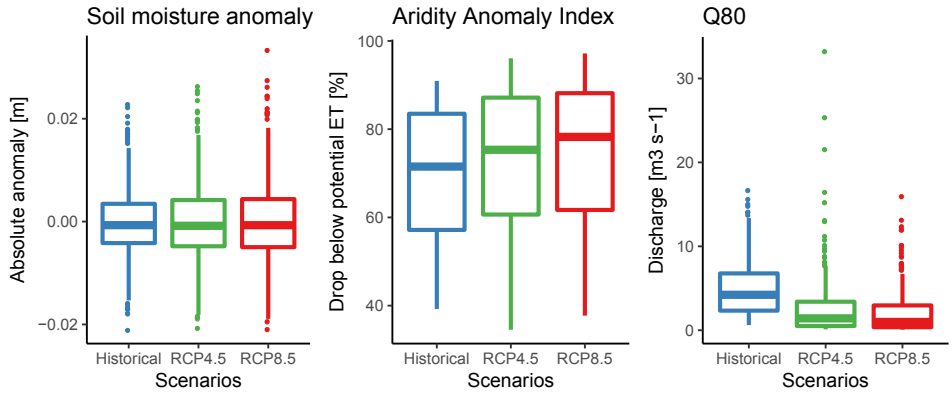

Figure 4.15: Distribution of drought indices under the historical climate (same as in figure 4.6) and under RCP4.5 and RCP8.5 with projected AquaCrop irrigation water requirements (Approach 3). All indices are monthly and spatial averages for the basin.

the global rules, detailed allocation and adaptation strategies are lost.

The regional analysis is presented in figure 4.15. For the basin on average, droughts occur more often than historically. The soil moisture anomaly distributions become wider, meaning that the extreme wetness and extreme dryness in the top soil store increase. Looking at the Aridity Anomaly Index however, the wetness will occur less (even though it may be more extreme), because the AAI quartiles do not widen but heighten. It means that water limitation of actual evaporation causes progressively larger agricultural dryness under RCP4.5 and RCP8.5. The low flow (Q80) of the extremely wet years (dots in the right panel) will remain unchanged (RCP4.5 even shows wetter years than historically) but overall, the median of the distribution shifts and hydrological drought will be more pronounced.

The regional downstream consequences of irrigation (including the AquaCrop requirements for Tadla) can be deducted from figure 4.16, by looking at the difference between the upstream discharge stations: Dechra El Oued and Mechra Eddahk, and the outlet. For the former two, the median discharge in winter decreases more than in spring and summer. This follows from the projection of less precipitation in winter and from the fact that summer flows are already low. At the outlet however, discharge decreases more consistently over the year, because here the spatial effects of irrigation requirements are felt: the withdrawals, that are especially concentrated in summer, are included on top of the climatic change. It can be seen that RCP8.5 is a clearly drier scenario for these months. This projection opposes a similar analysis of median discharge made in the MOSAICC project (Balaghi et al., 2016) with the hydrological model STREAM. Instead of the seasonal pattern, their decrease in unregulated discharge seemed to be a constant 70-50 percent for 2010-2040. The difference is likely the result of model differences and the current inclusion of reservoir operation and withdrawals.

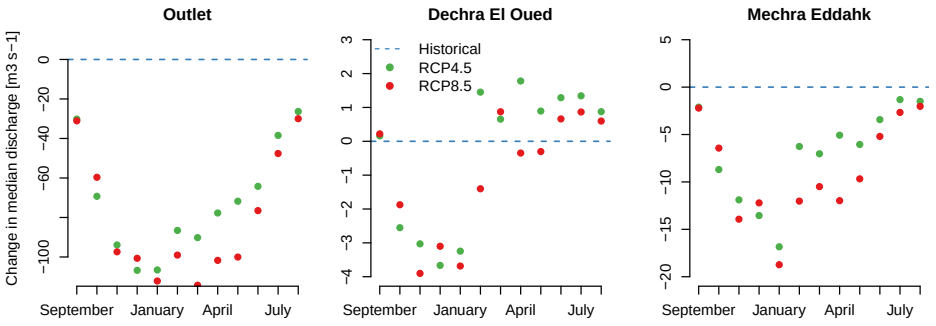

Figure 4.16: Average change in median discharge under RCP4.5 and 8.5, at the two stations with highest efficiency and the basin's outlet. Calculated for 2020-2050 and Approach 3. The metric signifies discharge with a 50 percent chance of exceedance.

Chapter 5

Discussion

In three ways the large scale hydrological model was combined (had its irrigation routine replaced) with the simulations of AquaCrop. During those three replacements, several human influences that shape the impact of climate change or increased water use, were expressed. For instance the transfer to Tessaout-Aval, the inter-crop prioritization and the crop specific groundwater contribution. These extensions made the hydrological and agricultural impact assessments more coupled than the studies previously conducted in the basin. MOSAICC for instance assesses surface water resources only as discharge free from human regulation, and has no link between these surface water resources and crop growth. The latter concerns only the rainfed production. Whether the extensions in this study are helpful depends on how well they reflect the real human influence, but also on the reliability of hydrological- and crop modeling components.

5.1 Hydrological modeling

The accumulation of runoff to available surface water, was captured in reservoir storage. And with unprecedented minimums under RCP8.5, did the reservoirs that supply to Tadla behave as expected. But those supplying for instance to Haouz emptied from time to time in the historical analysis. They are situated in the smaller tributaries of the Oum Er Rbia river, where the operational scheme of PCR-GLOBWB has difficulty in handling the many small and large reservoirs. This behavior is undesired because only the Sidi Driss dam appears to have been empty once. Next to the operational rules however (see also section 5.3), deviations in reservoir storage may also follow from the model's local accumulation of runoff.

The upstream discharge estimates show more than 10 m^3s^{-1} bias for two of the four stations. The runoff-generation process in this karstic region of Dechra El Oued and Tarhat is dominated by lateral flows that are hard to capture in any cell-by-cell distributed hydrological model. The same

structure can be problematic in the Atlas mountains, close to the elevated Ait Ouchene station, where subsurface flows are poorly understood (Boulet et al., 2008).

Like in all hydrological assessments, imprecise runoff generation can be inherited from the meteorological input data (Biemans et al., 2009; Döll et al., 2016). This firstly can be an absence of signals: a measured precipitation trend in Tadla (Karrou et al., 2011, ch.2) seems to lack in the historical MSWEP set. But secondly, the meteorological forcing can be altered by the downscaling step, which is a recurrent obstacle in Moroccan climate impact studies (Balaghi et al., 2016; Gommes et al., 2008). The separate linear regression and lapse rate scaling of this study did not fully preserve the joined distribution of precipitation and temperature (Wilby and Wigley, 2000). Which can be influential for the snow pack dynamics in the Atlas mountains (Marchane et al., 2016). Still, regarding the meteorological and hydrological reliability for the Tadla case study, the model showed reliable discharge estimates for Mechra Eddahk, in the middle of the Tadla perimeter (figure 2.1). The future GFDL-ESM2M sets were confidently used because the CLIMDEX trends in winter/spring rainfall (table 4.2) are consistent with North-African and Moroccan multi-model projections (Dubrovskỳ et al., 2014; Driouech et al., 2010; Balaghi et al., 2016).

5.2 Crop modeling

The original irrigation routine of PCR-GLOBWB that was replaced, either outside or inside the water resources simulation, formed itself an underestimation of the reported historical surface water allocations (figure 4.7). The replacing calculations of AquaCrop in Approach 1 underestimated them by a similar magnitude and were quantitatively as good (or as bad). In this approach, the too small requirements originated from the represented average field and the upscaling procedure to Tadla-totals. Subsequently, as withdrawals, they barely lowered the accumulated water resources outside Tadla in PCR-GLOBWB. This caused the WSI to remain low, both through withdrawals (numerator) and the actual availability (denominator) (figures 4.9 and 4.13). In Approach 2 however, the accumulated water resources were the starting point. And the releases derived from them were much closer to the reported allocation than Approach 1 totals. Logically, after the downscaling, this also resulted in on-field applications that were relatively high (tables 4.1 and 4.3) and yields that especially for alfalfa, wheat and sugar beet could be higher than the designated 'good yield' of Approach 1 (table 3.3 and figure 4.10).

The higher yields could indicate that 'good yield' is picked from poor surveys. Because although the alfalfa target (20 t/ha) agrees with the survey of Sraïri et al. (2009), it is less than most yields reported for the calibration

experiments. And having a yield target less than achieved in experiments (i.e. under deliberate sub-optimal circumstances), means that unrealistically high stresses are tolerated and less water is required to reach the target. But if you suppose that the surveys are correct, and that large applications could be quite realistic, such as more than 1 meter of supplemental irrigation for alfalfa (Chahri and Saouabe, 2014), then the latter should not result in the high yields. It probably means that water use is too efficient in AquaCrop, even though the model simulates more sophisticated crop characteristics than PCR-GLOBWB and avoids the strong simplification of a rootzone that is instantaneously filled to field capacity (Wada et al., 2014; Nazemi and Wheater, 2015a).

First and most clearly were the Tadla requirements of Approach 1 underestimated because the exclusion of arboriculture implicitly said 'no irrigation water is needed in Tadla for citrus and olive trees'[1]. Still, the fact that all other dominant crops are considered is new, because previous studies in Tadla have often focused on reproducing small scale field experiments for one crop (Benabdelouahab et al., 2016; Addi, 2012). Secondly, the reference evapotranspiration of a meteorological reanalysis has a known influence on irrigation requirement models (Siebert and Döll, 2010), and could have prescribed too large rates to AquaCrop. One of its possible influences is that higher stresses are tolerated for the same amount of actual plant transpiration and production. Thirdly, the losses in the distribution network (assumed 0.2 (Zerouali, 2009)) and losses on the field, might have been larger. Zerouali (2009) and Kselik et al. (2008) state that the on-field application losses in Tadla are about 0.5. It is common to assume such a value (Jägermeyr et al., 2015) and when prescribed it immediately doubles the requirements. However, the strength of AquaCrop is that it explicitly simulates drainage of excess water from the rootzone through a physics-based approach[2]. But it does require that the flows in the profile are realistically represented. So fourthly, the chosen soil characteristics might not be representative enough. Their large influence on the experienced stress was already seen in the sensitivity analysis (figure 4.4). Soil 2 for instance raised the requirements for sugar beet heavily. And only then did the crop agree better with the range of the crop-factor approaches (Hennebert and Moerenhout, 2007; Akdim, 2014). Under Soil 1 it may be over-efficient.

Representativeness is an inherent issue of the aim to scale the general on-field situations of the four crops. It required that variability in many abiotic or human components was fixed. The act of irrigation for instance,

[1] In Approach 2, the parametric division does account for them. See Appendix D.

[2] Although physics-based, its combination with robta may lead to some underestimation. 15 Percent of the surface is bare in reality (with robta-canals and bunds (Hennebert and Moerenhout, 2007)), while it is planted in the model and has a rootzone. AquaCrop then overestimates the percolated water reaching the rootzones and underestimates requirements.

encounters heterogeneity in timing because farmers successively flood different parts (Benabdelouahab et al., 2016) and because ORMVAT delivers the water in Beni Amir rotationally (Karrou et al., 2011). Such intra-perimeter practices were forced to the three timing scenarios. Which for example caused the simulated alfalfa to fail in the known 1999-00 drought, because the fixed scheme did not assign water in the anomalous dry weeks that coincided with crop establishment, whereas in reality, with flexible irrigation, it did not fail completely (Balaghi et al., 2012; Ouraich et al., 2014; Ouassou et al., 2007). Some of the fixed heterogeneity in soil or timing could be varied again when the model is implemented on a grid (Lorite et al., 2013). Like the PCR-GLOBWB routine, that represents the 100,000 ha of the Tadla scheme with about 20 gridcells. But without the fictional crop. In Morocco this has been done before, for rainfed production at larger regional scales, with the WOFOST crop model (Balaghi et al., 2012) and in MOSAICC with AquaCrop (Balaghi et al., 2016).

Although the dynamic approach encountered difficulties in this very first application to irrigated crops for the whole of Tadla, it was able to produce the expected future sub-optimal conditions. Approach 2 showed for instance that all crops (sugarbeet and alfalfa last) become severely water limited under RCP8.5 (figure 4.14). Therefore, the crop modeling finds no need to resort to statistical methods. This is in contrast to a case study in Tunesia, where AquaCrop was found less scalable than rainfall-yield regression methods (Karrou et al., 2011, ch.10). In fact, the dynamic approach avoids the questionable assumption behind any regression: of a stationary relation between water and yield. It also provides a good argument against it: the yield projections of Approach 2 were under considerable influence of increased productivity by CO_2 fertilization. It favors AquaCrop over statistics, and also over the routines of large scale hydrological models that hardly incorporate this non-stationary effect (Döll et al., 2016).

5.3 Benefits of the multi-model approach

The growth of the irrigated crops was coupled to available water resources at different moments in the simulations[3]. Although the components performed reasonably, the deviation in them was transferred at each point. Approach 1 for instance underestimated water stress due to underestimated agricultural demands but possibly also due to an excess of accumulated water. And Approach 2 could overestimate production due to allocation of the same excess accumulation but also due to the discussed over-efficient water use. The coupling however has no precedent in the basin. Most earlier assessments focused on precipitation impacts in rainfed agriculture. And except

[3]Approach 1: after AquaCrop after PCR-GLOBWB. Approach 2: before AquaCrop, after PCR-GLOBWB. Approach 3: after AquaCrop, before PCR-GLOBWB.

MOSAICC, none have assessed the surface water resources. Although MOSAICC itself did not coupled the resource to any of its uses. Some studies did focus on irrigated agriculture, but for them the no-coupling is reversed: water resources were assumed to be unlimited (Gommes et al., 2008; Ouraich et al., 2014). But because there is no precedent it remains a question whether the extensions create an effect similar to the real human influence.

This was not always the case in the historical simulations. Here the accumulated resources in PCR-GLOBWB that were required for Approach 1 and 2, showed a rise after the Ahmed El Hansali dam reservoir constructed, which was unencountered in reality (Belghiti, 2009). This occurred because the accumulated 'surface water availability' needed to be coupled outside the simulation, and this cannot be done when the concept includes regular discharge. For example, at two perimeters downstream of each other, one would double-count water resources if the modeled streamflow passing in a time-span was summed. Some of the fictional accumulation upstream needs to be transferred and counted as accumulation downstream. Precisely this happens to the setup's reservoir storage, as it is subject to overflow in PCR-GLOBWB while the accumulation takes place. This desirable property was however imprecise, and required the moving window assumption to arrive at actual storage outside Tadla and to express the local impacts with WSI or yields.

This problem of spatio-temporal division of resources outside the simulation, was overcome in Approach 3. In this case it was done internally. Future AquaCrop requirements were directly linked to the daily PCR-GLOBWB water balance and its global allocation rules. But accordingly, explications of real human influences were lost, like the regional groundwater contributions and operational strategies. The prescription 'Ahmed El Hansali and Bin El Ouidane supply to Tadla, but only after the allocation to Tessaout Aval' reduced to the '600 km upstream'-rule[4]. This hinders the applicability for impact assessment, because for example the basin agency cannot test how much of stress is relieved when the primary allocation to Tessaout Aval is altered. Which makes the projections less useful (Cash et al., 2002). To still accommodate the local differences in operation, Nazemi and Wheater (2015b) suggest parametric approaches to reservoir operation. Although a fixed parameterization can deny the non-stationarity of operational decision making, it could prevent the empty reservoirs caused by global rules in this

[4]Besides the coarse nature of their allocation rules, another remark can be made about the pro- or retrospective operation schemes of the large scale models. Following mainstream economic theory, they contain a-priori expressions of how the water is allocated given a set of demands and resources. But in reality the contest for water depends on the possible impacts at these locations and not only on the local physical needs for water (as if they are blind to the availability-situation). ORMVAT for instance puts pressure on the basin agency when they foresee scarcity. In other words: operational demands are not the physical demands.

regional application. And if the parameters contain operational meaning it allows the operators to still search for adaptation strategies.

Seen from this perspective, a similar parametric approach was already taken in this study. Not at the basin scale however, but at the perimeter scale, to convert the total releases to irrigation on the average field, or the average field to the total requirements. This expression of ORMVAT's delivery, the prioritization of the crops and the farmers' timing, gave a major advantage over PCR-GLOBWB itself. While the original routine is based on one fictional crop that requires water but does not acquire biomass, the multi-model setup can explore adaptation strategies in terms of productivity. This ability for yield optimization was demonstrated with heightened wheat-prioritization under RCP4.5. Approaches 1 and 2 therefore come also closer to enabling other coupling effects on the agricultural use of water. Lionboui et al. (2014) for instance showed that price effects and drought can shift the groundwater contributions per crop, and thus the parameterization of this study (table D.1). A further separation into not only crop types, but also into common agronomic farm types (Sraïri et al., 2016; Akdim, 2014; Kwelde, 2006), could extend the current hydrological impacts to assessments of economic water productivity (Elame and Doukkali, 2012; Ouraich et al., 2014).

Chapter 6

Future research

Surface water for irrigation was extracted from regional hydrological simulations in PCR-GLOBWB. But for a still intertwined set of reasons, the hydrological performance was not good everywhere. An improved error detection is therefore recommended. For this, additional data is needed. (i) With in-situ measurements from the Direction Météorologie Nationale, and a subsequent run of PCR-GLOBWB, the meteorological differences between reanalysis- and in-situ-forcing are isolated. It would expose their contribution to hydrological deviation. (ii) As the modeling of discharge generating processes in the High Atlas may need improvement, the simulated snowpack should be validated. For this important regional source, remotely sensed products of snow cover already exist (Marchane et al., 2015). (iii) With the current four upstream stations it cannot be tested whether alterations propagate downstream and improve the applicability to other water use locations such as the perimeter of Doukkala. So downstream discharge observations need to be obtained.

It was established that the multi-model approaches inherit errors from the hydrological factors in PCR-GLOBWB and from forcing in both components. But they are also imprecise through the generalizations in soil and timing for AquaCrop. It is recommended to transform the influential aggregations of soil characteristics and irrigation schedules to a grid, like the crop modeling in the MOSAICC project (Balaghi et al., 2016). When this higher requirement for spatial information is met, more particularities within the perimeter can be represented. And when applied to this study's unique coupling to surface water availability, it can form the first, dynamic and more reliable model of Tadla's irrigated agriculture. Additionally, the model could be expanded and re-calibrated to incorporate the unexplained variation that currently lies in the implicit calibration to an average state of fertility, crop species and field management.

A parametric approach to reservoir operation, that fits better with reality in the heavily managed basin, can only be developed if basin agencies

grant access to data on reservoir levels and the data is collectively standardized. The model developers on their turn, should maintain an operational meaning in the approaches. Because the model will have more relevance for impact assessment if operational managers of ABHOER can alter the modeled allocation practices, see the water productivity consequences in the sectors and then collectively decide with the users such as ORMVAT what is most desired (Cash et al., 2002). A potential lies in collaboration with MOSAICC because their employed STREAM model does not yet include regulation, but in the near future it probably will. Its way will conceptually differ from the prospective schemes of PCR-GLOBWB, and forms an opportunity to test and compare.

The updating of withdrawals and resources in Approaches 1 and 2, outside the large scale model, was only possible by assuming a moving window. Approach 3 did not have this problem. But upon replacing the requirements of the original irrigation routine, it lacked a return flow from the soil profile, whereas in reality the amount of percolated irrigation water is high (Kselik et al., 2008). Additionally, it lost the ability to specify detailed allocation rules. The recommended way forward is to embed the in- and output of AquaCrop inside the large scale model, so productivity is expressed and irrigation schedules are directly linked to the modeled water balance. Although this requires a high amount of operational information, the efforts would be of interest to the 'hyper resolution' community. Their research line builds on the expectation that the improvement of remote sensing, parameterization sets and forcing products will soon enable highly detailed distributed models (Bierkens et al., 2015). However, these improvements concern mostly physical hydrological processes, while the representation of the operational ones is just as challenging. Consider for instance the case where the Tadla perimeter is suddenly represented by 10.000 gridcells (10 ha each); In what structure can the rotational delivery with different crop priorities, that transfers water between all cells, be resolved? And how to describe it such that the adaptive strength of a new operational strategy can be tested?

Chapter 7

Conclusions

The Oum Er Rbia basin was modeled in regional runs of the large scale hydrological model PCR-GLOBWB. At the Mechra Eddahk discharge station, located in the Tadla perimeter case study, streamflow observations were well reproduced. Compared to the allocation reports however, the original irrigation routine of PCR-GLOBWB underestimated the total surface water withdrawals in the perimeter. Next to the desire for detailed irrigation modeling, this provided another reason to test its replacement with AquaCrop in one of the three multi-model approaches. In Approach 1 and 2, PCR-GLOBWB therefore only accumulated the resources available to Tadla, that were externally coupled to the irrigation. But because of the moving window assumption this didn't guarantee a closed water balance. So further attempts to couple after the separate simulations are not advised.

Still, the illustration was continued. Because inside the irrigated perimeter, the AquaCrop model dynamically related water to productive crop growth of the four dominant crops. Upon validation it reproduced the specific situations well (R^2= 0.45 to 0.99) and with fixed factors it represented the average situations of the crops. These were on their turn scaled with crop abundances, inter-crop prioritization and groundwater contributions, and became valuable for the two metrics of local climate impacts: water stresses with high temporal resolution and crop productivity. The former can consider patterns of stress to optimize allocation of water to agriculture. The latter can take this allocated amount as limitation and optimize biophysical production. It for instance showed that wheat yields can be enlarged by a different prioritization of crops: whereas maize is the most water consuming one, alfalfa and sugarbeet are hardly water limited. They easily achieve their potentials (currently and in RCP4.5) and can miss some irrigation. So if ORMVAT wants to ration or redistribute the applied water, it could start with these two crops. Whether this is economically viable, is easily determined with an agronomic extension of the model.

In the study area description it was already established that the current

use of the groundwater resources in the perimeter is unsustainable. Extra care thus needs to be taken with the rigid agriculture that this study assumed. The assumed equal future ground water contribution will not occur when the institutions implement the advised limitation of groundwater use. This will enlarge this study's projected impacts on surface water resources.

These projections for the future were made for multiple aspects of the water-agricultural system. The forcing projects a meteorological drying of the region. Average rainfall in winter and spring will decrease, periods of dryness will lengthen and rainfall becomes more extreme when it occurs. Multiple simulations for 2020-2050 showed that the basin's hydrological regime and agricultural productivity will be affected. Approach 1 showed dropping actual reservoir storages under RCP8.5. Which results in rising water stresses for Tadla that reach their maximum in summer. This coincides with the growing season of maize and its corresponding high requirements. Approach 2 lay more in line with the historical release statistics than Approach 1. It constructed a future availability per crop by explicit reservoir operation and a parametric division between the crops, and prescribed it to AquaCrop. Under RCP4.5 this showed that water limitation only occurs for maize and wheat, meaning that yields of alfalfa and sugar beet increase by CO_2 fertilization. But for RCP8.5 the drop in actual storage started to limit all crops, with an occasional failure of harvest. At this stage RCP8.5 clearly becomes the scenario where possible benefits for crop growth (the fertilization) are outweighed by the decline in water resources and a large year to year variation.

At the basin scale, the climate change impacts on water resources and on irrigation were coupled in Approach 3. As expected, the interconnected impacts are pronounced. RCP4.5 and 8.5 showed a progressive increase in extreme soil moisture anomalies, in water limitation of actual evapotranspiration and in low discharges during hydrological drought. The results imply that the water system is likely easier to regulate under the RCP4.5 scenario and can possibly sustain more use. These three indicators, that successfully reflect different stages of drought, can complement the existing operational monitoring (Ouassou et al., 2007; Pozzi et al., 2013).

So, Yes. Water resources assessment was improved with the multi-model approach. It elaborated upon the existing projections for the region and explored through its three different couplings, how the interconnections that shape climate impacts in Oum Er Rbia, can be better expressed.

Bibliography

Addi, M. (2012). Calage et validation de modèle cropsyst et son utilisation pour le bersim au tadla. Insitut Agronomique et Vétérinaire Hassan II.

Agence du Bassin Hydraulique de l'Oum Er Rbia (2007). Ressources en eau du bassin d'oum er rbia: Quelle gestion adoptée face aux changements climatiques? In *Conférence internationale sur l'application de la Directive Cadre Européenne sur l'Eau*.

Agence du Bassin Hydraulique de l'Oum Er Rbia (2010). Pour une gestion intgrée, concertée, et participative des ressources en eau dans le bassin de l'oum er rbia. In *Programme Appui à la Gestion Intégrée des Ressources en Eau*.

Agence du Bassin Hydraulique de l'Oum Er Rbia (2012). Projet de plan directeur daménagement intégré des ressources en eau du bassin de loum er rbia et des bassins côtiers atlantiques. Technical report.

Ahmadi, S. H., Mosallaeepour, E., Kamgar-Haghighi, A. A., and Sepaskhah, A. R. (2015). Modeling maize yield and soil water content with aquacrop under full and deficit irrigation managements. *Water Resources Management*, 29(8):2837–2853.

Akdim, K. (2014). Systèmes de culture et valorisation de l'eau d'irrigation dans le bassin versant d'oum rbia (région de tadla-azilal). Insitut Agronomique et Vétérinaire Hassan II.

Alexander, L., Zhang, X., Peterson, T., Caesar, J., Gleason, B., Klein Tank, A., Haylock, M., Collins, D., Trewin, B., Rahimzadeh, F., et al. (2006). Global observed changes in daily climate extremes of temperature and precipitation. *Journal of Geophysical Research: Atmospheres*, 111(D5).

Alexandratos, N., Bruinsma, J., et al. (2012). World agriculture towards 2030/2050: the 2012 revision. Technical report, ESA Working paper Rome, FAO.

Alishiri, R., Paknejad, F., Aghayari, F., et al. (2014). Simulation of sugarbeet growth under different water regimes and nitrogen levels by aqua crop. *International Journal of Biosciences (IJB)*, 4(4):1–9.

Allen, R. G., Pereira, L. S., Raes, D., Smith, M., et al. (1998). Crop evapotranspiration-guidelines for computing crop water requirements - fao irrigation and drainage paper 56. *FAO, Rome*, 300(9):D05109.

Arnell, N. W. and Lloyd-Hughes, B. (2014). The global-scale impacts of climate change on water resources and flooding under new climate and socio-economic scenarios. *Climatic Change*, 122(1-2):127–140.

Balaghi, R., El Hairech, T., Alaouri, M., Moutaouakkil, S., Benabdelouahab, T., Mounir, F., Lahlou, M., Arrach, R., Abderrafik, M., Colmant, R., Evangelisti, M., Poortinga, A., Kuik, O., and Delobel, F. (2016). Climate change impact assessment using mosaicc in morocco. *INRA, Maroc*.

Balaghi, R., Jlibene, M., Tychon, B., and Eerens, H. (2012). La prédiction agrométéorologique des rendements céréaliers au maroc. *INRA, Maroc*.

Beck, H. E., van Dijk, A. I. J. M., Levizzani, V., Schellekens, J., Miralles, D. G., Martens, B., and de Roo, A. (2016). Mswep: 3-hourly 0.25 degree global gridded precipitation (1979–2015) by merging gauge, satellite, and reanalysis data. *Hydrology and Earth System Sciences Discussions*, 2016:1–38.

Bekkar, Y., Kuper, M., Hammani, A., Dionnet, M., and Eliamani, A. (2007). Reconversion vers des systèmes dirrigation localisée au maroc quels enseignements pour lagriculture familiale. *Hommes, terre et eaux*, 137:7–20.

Belghiti, M. (2009). Le plan national d'econmomie d'eau en irrigation (pneei): une réspone au défi de la raréfaction des ressources en eau. In *Confrérence Inter Rrégionale Enviro Water*.

Benabdelouahab, T., Balaghi, R., Hadria, R., Lionboui, H., Djaby, B., and Tychon, B. (2016). Testing aquacrop to simulate durum wheat yield and schedule irrigation in a semi-arid irrigated perimeter in morocco. *Irrigation and Drainage*.

Benabdelouahab, T., Balaghi, R., Hadria, R., Lionboui, H., Minet, J., and Tychon, B. (2015). Monitoring surface water content using visible and short-wave infrared spot-5 data of wheat plots in irrigated semi-arid regions. *International Journal of Remote Sensing*, 36(15):4018–4036.

Bennani, A., Buret, J., and Senhaji, F. (2001). Communication nationale initiale a la convention cadre des nations unies sur les changements climatiques. Technical report, Ministere de l'Amenagement du Territoire, de l'Urbanisme de l'Habitat et de l'Environnement.

Bergström, S. (1976). Development and application of a conceptual runoff model for scandinavian catchments. Technical report, SMHI.

Bergström, S., Singh, V., et al. (1995). The hbv model. *Computer models of watershed hydrology*, pages 443–476.

Biemans, H., Haddeland, I., Kabat, P., Ludwig, F., Hutjes, R., Heinke, J., Von Bloh, W., and Gerten, D. (2011). Impact of reservoirs on river discharge and irrigation water supply during the 20th century. *Water Resources Research*, 47(3).

Biemans, H., Hutjes, R., Kabat, P., Strengers, B., Gerten, D., and Rost, S. (2009). Effects of precipitation uncertainty on discharge calculations for main river basins. *Journal of Hydrometeorology*, 10(4):1011–1025.

Bierkens, M. F. (2015). Global hydrology 2015: State, trends, and directions. *Water Resources Research*, 51(7):4923–4947.

Bierkens, M. F., Bell, V. A., Burek, P., Chaney, N., Condon, L. E., David, C. H., de Roo, A., Döll, P., Drost, N., Famiglietti, J. S., et al. (2015). Hyper-resolution global hydrological modelling: what is next? everywhere and locally relevant. *Hydrol Process*, 29(2):310–320.

Bos, M. G. et al. (1989). *Discharge measurement structures*. International Institute for Land Reclamation and Improvement.

Bouazzama, B., Xanthoulis, D., Bouaziz, A., Ruelle, P., and Mailhol, J.-C. (2012). Effect of water stress on growth, water consumption and yield of silage maize under flood irrigation in a semi-arid climate of tadla (morocco). *Biotechnologie, Agronomie, Société et Environnement*, 16(4):468.

Boulet, G., Boudhar, A., Hanich, L., Duchemin, B., Simonneaux, V., Maisongrande, P., Chehbouni, A., Thomas, S., and Chaponniere, A. (2008). Hydrological modelling in the high atlas mountains with the help of remote-sensing data: milestones of the sudmed project. In *13th IWRA World Water Congress*, pages 1–4.

Box, G. E., Jenkins, G. M., Reinsel, G. C., and Ljung, G. M. (2015). *Time series analysis: forecasting and control*. John Wiley & Sons.

Brauman, K. A., Richter, B. D., Postel, S., Malsy, M., and Flörke, M. (2016). Water depletion: An improved metric for incorporating seasonal and dry-year water scarcity into water risk assessments. *Elementa: Science of the Anthropocene*, 4(1):000083.

Bredehoeft, J. D. (2002). The water budget myth revisited: why hydrogeologists model. *Groundwater*, 40(4):340–345.

Campbell, G. S. (1974). A simple method for determining unsaturated conductivity from moisture retention data. *Soil science*, 117(6):311–314.

Cash, D., Clark, W. C., Alcock, F., Dickson, N. M., Eckley, N., and Jäger, J. (2002). Salience, credibility, legitimacy and boundaries: Linking research, assessment and decision making.

Chahri, R. and Saouabe, T. (2014). La reconversion collective à l'irrigation localisée dans le tadla : Analyse de l'approche de l'équipement interne et impact sur les pr'él'évements à partir de la nappe. Insitut Agronomique et Vétérinaire Hassan II.

Chaponniere, A. and Smakhtin, V. (2006). *A review of climate change scenarios and preliminary rainfall trend analysis in The Oum er Rbia Basin, Morocco*, volume 110. IWMI.

Choluj, D., Karwowska, R., Jasinska, M., and Haber, G. (2004). Growth and dry matter partitioning in sugar beet plants (beta vulgaris l.) under moderate drought. *Plant, Soil and Environment*, 50(6):265–272.

Clapp, R. B. and Hornberger, G. M. (1978). Empirical equations for some soil hydraulic properties. *Water resources research*, 14(4):601–604.

Cook, B. I., Anchukaitis, K. J., Touchan, R., Meko, D. M., and Cook, E. R. (2016). Spatiotemporal drought variability in the mediterranean over the last 900 years. *Journal of Geophysical Research: Atmospheres*.

Dadson, S., Acreman, M., and Harding, R. (2013). Water security, global change and land–atmosphere feedbacks. *Phil. Trans. R. Soc. A*, 371(2002):20120412.

Dai, A. (2011). Drought under global warming: a review. *Wiley Interdisciplinary Reviews: Climate Change*, 2(1):45–65.

Döll, P., Douville, H., Güntner, A., Schmied, H. M., and Wada, Y. (2016). Modelling freshwater resources at the global scale: Challenges and prospects. In *Remote Sensing and Water Resources*, pages 5–31. Springer.

Döll, P., Fritsche, M., Eicker, A., and Schmied, H. M. (2014). Seasonal water storage variations as impacted by water abstractions: comparing the output of a global hydrological model with grace and gps observations. *Surveys in Geophysics*, 35(6):1311–1331.

Doorenbos, J. and Kassam, A. (1979). Yield response to water- fao irrigation and drainage paper 33. *FAO, Rome*, 33:257.

Doukkali, M. (2005). Water institutional reforms in morocco. *Water Policy*, 7(1):71–88.

Driouech, F. (2010). *Distribution des précipitations hivernales sur le Maroc dans le cadre d'un changement climatique: descente d'échelle et incertitudes*. INPT.

Driouech, F., Déqué, M., and Mokssit, A. (2009). Numerical simulation of the probability distribution function of precipitation over morocco. *Climate dynamics*, 32(7-8):1055–1063.

Driouech, F., Déqué, M., and Sánchez-Gómez, E. (2010). Weather regimes-moroccan precipitation link in a regional climate change simulation. *Global and Planetary Change*, 72(1):1–10.

Dubrovskỳ, M., Hayes, M., Duce, P., Trnka, M., Svoboda, M., and Zara, P. (2014). Multi-gcm projections of future drought and climate variability indicators for the mediterranean region. *Regional Environmental Change*, 14(5):1907–1919.

Dunne, J. P., John, J. G., Adcroft, A. J., Griffies, S. M., Hallberg, R. W., Shevliakova, E., Stouffer, R. J., Cooke, W., Dunne, K. A., Harrison, M. J., et al. (2012). Gfdl's esm2 global coupled climate-carbon earth system models. part i: Physical formulation and baseline simulation characteristics. *Journal of Climate*, 25(19):6646–6665.

eartH2Observe (2014). Deliverable no: D.2.3 review of stakeholders, relevant policies in non-european case study river basins. Technical report.

eartH2Observe (2015). Deliverable no: D.5.1 report on the current state-of-the-art water resources reanalysis (wrr1-tier 1). Technical report.

Ekström, M., Grose, M. R., and Whetton, P. H. (2015). An appraisal of downscaling methods used in climate change research. *Wiley Interdisciplinary Reviews: Climate Change*, 6(3):301–319.

El Jihad, M. D. (2003). Les sécheresses saisonnières dans le haut bassin de l oum-er-rbia (maroc central): aspects et fréquences. *Science et changements planétaires/Sécheresse*, 14(3):157–167.

Elame, F. and Doukkali, R. (2012). Water valuation in agriculture in the souss-massa basin (morocco). In *Integrated Water Resources Management in the Mediterranean Region*, pages 109–122. Springer.

Elliott, J., Deryng, D., Müller, C., Frieler, K., Konzmann, M., Gerten, D., Glotter, M., Flörke, M., Wada, Y., Best, N., et al. (2014). Constraints and potentials of future irrigation water availability on agricultural production under climate change. *Proceedings of the National Academy of Sciences*, 111(9):3239–3244.

Falkenmark, M., Berntell, A., Jägerskog, A., Lundqvist, J., Matz, M., and Tropp, H. (2007). *On the verge of a new water scarcity: a call for good governance and human ingenuity*. Stockholm International Water Institute (SIWI).

Faysse, N., Errahj, M., Kuper, M., and Mahdi, M. (2010). Learning to voice? evolving roles of family farmers in the coordination of large-scale irrigation schemes in morocco. *Water alternatives*, 3(1):48.

Flörke, M., Kynast, E., Bärlund, I., Eisner, S., Wimmer, F., and Alcamo, J. (2013). Domestic and industrial water uses of the past 60 years as a mirror of socio-economic development: A global simulation study. *Global Environmental Change*, 23(1):144–156.

Food and Agriculture Organisation of the United Nations (2014). Dams of morocco. data retrieved from AQUASTAT: `http://www.fao.org/nr/water/aquastat/countries_regions/MAR/index.stm`.

Food and Agriculture Organisation of the United Nations (2016). Faostat 2016: Fao statistical databases. data retrieved from: `http://www.fao.org/faostat/en/#data`.

García-Vila, M. and Fereres, E. (2012). Combining the simulation crop model aquacrop with an economic model for the optimization of irrigation management at farm level. *European Journal of Agronomy*, 36(1):21–31.

Gommes, R., El Hairech, T., Rosillon, D., Balaghi, R., and Kanamaru, H. (2008). Impact of climate change on agricultural yields in morocco. Technical report. World Bank.

Hagemann, S. (2002). *An improved land surface parameter dataset for global and regional climate models*. Max-Planck-Institut für Meteorologie.

Hagemann, S. and Gates, L. D. (2003). Improving a subgrid runoff parameterization scheme for climate models by the use of high resolution data derived from satellite observations. *Climate Dynamics*, 21(3-4):349–359.

Hennebert, D. and Moerenhout, T. (2007). *Conflict between water demand and supply in the Tadla irrigation scheme (Morocco) : Actual situation and future trends*. Vrije Universiteit Brussel.

Hunink, J. and Droogers, P. (2011). Climate change impact assessment on crop production in uzbekistan. *World Bank Study on Reducing Vulnerability to Climate Change in Europe and Central Asia (ECA) Agricultural Systems. Report FutureWater*, 106.

Jägermeyr, J., Gerten, D., Heinke, J., Schaphoff, S., Kummu, M., and Lucht, W. (2015). Water savings potentials of irrigation systems: global simulation of processes and linkages. *Hydrology and Earth System Sciences*, 19(7):3073–3091.

Jarvis, A., Reuter, H., Nelson, A., and Guevara, E. (2008). Hole-filled seamless srtm data v4. *International Centre for Tropical Agriculture (CIAT)*. data retrieved from: `http://srtm.csi.cgiar.org`.

Karrou, M., Bahri, A., and Oweis, T. (2014). Improvement of conjunctive use of green and blue waters through the development and promotion of supplemental irrigation in rainfed areas of west asia and north africa. *Community-Based Optimization of the Management of Scarce Water Resources in Agriculture*. International Center for Agricultural Research in Dry Areas, Benchmark project Phase 2.

Karrou, M., Oweis, T., and Bahri, A. (2011). Improving water and land productivities in rainfed systems. *Community-Based Optimization of the Management of Scarce Water Resources in Agriculture*, 8. International Center for Agricultural Research in Dry Areas, Benchmark project Phase 1.

Kiguchi, M., Shen, Y., Kanae, S., and Oki, T. (2015). Re-evaluation of future water stress due to socio-economic and climate factors under a warming climate. *Hydrological Sciences Journal*, 60(1):14–29.

Kim, D. (2015). *Agricultural Water Management in the Sevier River Basin, Utah: A Multidisciplinary Approach*. Utah State University.

Kim, D. and Kaluarachchi, J. (2015). Validating fao aquacrop using landsat images and regional crop information. *Agricultural Water Management*, 149:143–155.

Kornelsen, K. C. and Coulibaly, P. (2013). Advances in soil moisture retrieval from synthetic aperture radar and hydrological applications. *Journal of Hydrology*, 476:460–489.

Kraijenhoff Van De Leur, D. (1958). A study of non-steady groundwater flow with special reference to a reservoir-coefficient. *De Ingenieur*, 70(19):87–94.

Kselik, R. A., Bos, M. G., Hammani, A., and Bellouti, A. (2008). Assessment of sustainable agriculture in the irrigated perimeter of tadla, morocco using the criwar strategy module. In *IWRA Conference paper*.

Kummu, M., Ward, P. J., de Moel, H., and Varis, O. (2010). Is physical water scarcity a new phenomenon? global assessment of water shortage over the last two millennia. *Environmental Research Letters*, 5(3):034006.

Kuper, M., Hammani, A., Chohin, A., Garin, P., and Saaf, M. (2012). When groundwater takes over: linking 40 years of agricultural and groundwater dynamics in a large-scale irrigation scheme in morocco. *Irrigation and drainage*, 61(S1):45–53.

Kwelde, M. (2006). Suivi des explorations agricoles du tadla en vue de determenier leurs perfrmances dans l'utilisation des aux souterraines. Insitut Agronomique et Vétérinaire Hassan II.

Lange, S. (2016). Isimip2b bias correction fact sheet. retrieved from: `https://www.isimip.org/documents/112/ISIMIP2b_biascorrection_factsheet_s4SRaGe.pdf`.

Lehner, B., Liermann, C. R., Revenga, C., Vörösmarty, C., Fekete, B., Crouzet, P., Döll, P., Endejan, M., Frenken, K., Magome, J., et al. (2011). High-resolution mapping of the world's reservoirs and dams for sustainable river-flow management. *Frontiers in Ecology and the Environment*, 9(9):494–502.

Lionboui, H., Fadlaoui, A., Elame, F., and Benabdelouahab, T. (2014). Water pricing impact on the economic valuation of water resources. *International Journal of Education and Research*, 2(6):147–166.

Liu, Y., Dorigo, W. A., Parinussa, R., de Jeu, R. A., Wagner, W., McCabe, M. F., Evans, J., and Van Dijk, A. (2012). Trend-preserving blending of passive and active microwave soil moisture retrievals. *Remote Sensing of Environment*, 123:280–297.

López López, P., Wanders, N., Schellekens, J., Renzullo, L. J., Sutanudjaja, E. H., and Bierkens, M. F. (2016). Improved large-scale hydrological modelling through the assimilation of streamflow and downscaled satellite soil moisture observations. *Hydrology and Earth System Sciences*, 20(7):3059–3076.

Lorite, I., García-Vila, M., Santos, C., Ruiz-Ramos, M., and Fereres, E. (2013). Aquadata and aquagis: two computer utilities for temporal and spatial simulations of water-limited yield with aquacrop. *Computers and electronics in agriculture*, 96:227–237.

Marchane, A., Jarlan, L., Boudhar, A., Tramblay, Y., and Hanich, L. (2016). Linkages between snow cover, temperature and rainfall and the north atlantic oscillation over morocco. *Climate Research*, 69(3):229–238.

Marchane, A., Jarlan, L., Hanich, L., Boudhar, A., Gascoin, S., Tavernier, A., Filali, N., Le Page, M., Hagolle, O., and Berjamy, B. (2015). Assessment of daily modis snow cover products to monitor snow cover dynamics over the moroccan atlas mountain range. *Remote Sensing of Environment*, 160:72–86.

Martens, B., Miralles, D. G., Lievens, H., van der Schalie, R., de Jeu, R. A., Fernández-Prieto, D., Beck, H. E., Dorigo, W. A., and Verhoest, N. E. (2016). Gleam v3: satellite-based land evaporation and root-zone soil moisture. *Geoscientific Model Development Discussions*, pages 1–36. in review.

Mekonnen, M. M. and Hoekstra, A. Y. (2016). Four billion people facing severe water scarcity. *Science advances*, 2(2):e1500323.

Milewski, A., Elkadiri, R., and Durham, M. (2015). Assessment and comparison of tmpa satellite precipitation products in varying climatic and topographic regimes in morocco. *Remote Sensing*, 7(5):5697–5717.

Ministre de l'Energie, des Mines, de l'Eau et de l'Environnement (2015). Mobilisation de eaux de surface: grands barrages réalises. data retrieved from: `http://www.water.gov.ma/wp-content/uploads/2015/12/Liste_barrages_realises.pdf`.

Mohamed, Y., Van den Hurk, B., Savenije, H., and Bastiaanssen, W. (2005). Hydroclimatology of the nile: results from a regional climate model. *Hydrology and Earth System Sciences Discussions*, 2(1):319–364.

Moss, R. H., Edmonds, J. A., Hibbard, K. A., Manning, M. R., Rose, S. K., Van Vuuren, D. P., Carter, T. R., Emori, S., Kainuma, M., Kram, T., et al. (2010). The next generation of scenarios for climate change research and assessment. *Nature*, 463(7282):747–756.

Müller Schmied, H., Eisner, S., Franz, D., Wattenbach, M., Portmann, F. T., Flörke, M., and Döll, P. (2014). Sensitivity of simulated global-scale freshwater fluxes and storages to input data, hydrological model structure, human water use and calibration. *Hydrology and Earth System Sciences*, 18(9):3511–3538.

Mzibra, A., Zehauf, M., and Douira, A. (2008). Effet du cycle de la culture sur le rendement qualitatif et quantitatif de la betterave sucrière dans la région du gharb (maroc). *Biotechnologie, Agronomie, Société et Environnement*, 12(2):139–146.

Nazemi, A. and Wheater, H. S. (2015a). On inclusion of water resource management in earth system models–part 1: Problem definition and representation of water demand. *Hydrology and Earth System Sciences*, 19(1):33–61.

Nazemi, A. and Wheater, H. S. (2015b). On inclusion of water resource management in earth system models–part 2: Representation of water supply and allocation and opportunities for improved modeling. *Hydrology and Earth System Sciences*, 19(1):63–90.

Nejjam, I. (2013). Substitution partielle de la luzerne par de l'ensilage de maïs au périmètre irrigué de tadla: performances laitières, valorisation de l'eau d'irrigation et intérêt économique. Insitut Agronomique et Vétérinaire Hassan II.

New, M., Lister, D., Hulme, M., and Makin, I. (2002). A high-resolution data set of surface climate over global land areas. *Climate research*, 21(1):1–25.

Nyakudya, I. W. and Stroosnijder, L. (2014). Effect of rooting depth, plant density and planting date on maize (zea mays l.) yield and water use efficiency in semi-arid zimbabwe: Modelling with aquacrop. *Agricultural Water Management*, 146:280–296.

Ouassou, A., Ameziane, T., Ziyad, A., Belghiti, M., et al. (2007). Application of the drought management guidelines in morocco. *Options Méditerranéennes, Series B*, (58):343–372.

Ouraich, I., Tyner, W. E., et al. (2014). Climate change impacts on moroccan agriculture and the whole economy: An analysis of the impacts of the plan maroc vert in morocco. Technical report. WIDER Working Paper, No. 2014/083.

Ouzemou, J. E., El Harti, A., Moujahid, A. E., Bouch, N., El Ouazzani, R., Lhissou, R., and Bachaoui, E. M. (2015). Mapping crop based on phenological characteristics using time-series ndvi of operational land imager data in tadla irrigated perimeter, morocco. In *SPIE Remote Sensing*, pages 96372G–96372G. International Society for Optics and Photonics.

Pahl-Wostl, C. (2007). Transitions towards adaptive management of water facing climate and global change. *Water resources management*, 21(1):49–62.

Petitguyot, T. and Rieu, T. (2006). How more regulated dam release can improve the supply from groundwater and surface water in the tadla irrigation scheme in morocco. In *Water Governance for Sustainable Development*, pages 205–222.

Porporato, A., Laio, F., Ridolfi, L., and Rodriguez-Iturbe, I. (2001). Plants in water-controlled ecosystems: active role in hydrologic processes and response to water stress: Iii. vegetation water stress. *Advances in Water Resources*, 24(7):725–744.

Portmann, F. T., Siebert, S., and Döll, P. (2010). Mirca2000global monthly irrigated and rainfed crop areas around the year 2000: A new high-resolution data set for agricultural and hydrological modeling. *Global Biogeochemical Cycles*, 24(1).

Postel, S. L., Daily, G. C., Ehrlich, P. R., et al. (1996). Human appropriation of renewable fresh water. *Science-AAAS-Weekly Paper Edition*, 271(5250):785–787.

Pozzi, W., Sheffield, J., Stefanski, R., Cripe, D., Pulwarty, R., Vogt, J. V., Heim Jr, R. R., Brewer, M. J., Svoboda, M., Westerhoff, R., et al. (2013). Toward global drought early warning capability: Expanding international cooperation for the development of a framework for monitoring and forecasting. *Bulletin of the American Meteorological Society*, 94(6):776–785.

Raes, D., Steduto, P., Hsiao, T. C., and Fereres, E. (2012). Aquacrop. *Reference Manual*.

Ritchie, J. T. (1972). Model for predicting evaporation from a row crop with incomplete cover. *Water resources research*, 8(5):1204–1213.

Roerink, G., Jacobs, C., and Hammani, A. (2009). Assessment of groundwater extraction in the tadla irrigated perimeter (morocco) using the ssebi remote sensing algorithm. In *23rd European Regional Conference of the ICID*, pages 18–24.

Schneider, U., Becker, A., Finger, P., Meyer-Christoffer, A., Rudolf, B., and Ziese, M. (2011). Gpcc full data reanalysis version 6.0 at 0.5: monthly land-surface precipitation from rain-gauges built on gts-based and historic data.

Schrier, G., Barichivich, J., Briffa, K., and Jones, P. (2013). A scpdsi-based global data set of dry and wet spells for 1901–2009. *Journal of Geophysical Research: Atmospheres*, 118(10):4025–4048.

Siebert, S. and Döll, P. (2010). Quantifying blue and green virtual water contents in global crop production as well as potential production losses without irrigation. *Journal of Hydrology*, 384(3):198–217.

Sloan, P. G. and Moore, I. D. (1984). Modeling subsurface stormflow on steeply sloping forested watersheds. *Water Resources Research*, 20(12):1815–1822.

Sperna Weiland, F., Lopez, P., Van Dijk, A., and Schellekens, J. (2015). Global high-resolution reference potential evaporation. In *MODSIM 2015, Conference Proceedings*.

Sperna Weiland, F., Van Beek, L., Kwadijk, J., and Bierkens, M. (2012). Global patterns of change in discharge regimes for 2100. *Hydrology and Earth System Sciences*, 16:1047–1062.

Sraïri, M. T., Benjelloun, R., Karrou, M., Ates, S., and Kuper, M. (2016). Biophysical and economic water productivity of dual-purpose cattle farming. *animal*, 10(02):283–291.

Sraïri, M. T., Rjafallah, M., Kuper, M., and Le Gal, P.-Y. (2009). Water productivity through dual purpose (milk and meat) herds in the tadla irrigation scheme, morocco. *Irrigation and Drainage*, 58(S3).

Steduto, P., Hsiao, T., Fereres, E., and Raes, D. (2012). Crop yield response to water - fao irrigation and drainage paper 66. *FAO, Rome*, 66.

Steduto, P., Raes, D., Hsiao, T., Fereres, E., Heng, L., Izzi, G., and Hoogeveen, J. (2009). Aquacrop: a new model for crop prediction under water deficit conditions. *FAO, Rome*.

Stephens, E., Day, J. J., Pappenberger, F., and Cloke, H. (2015). Precipitation and floodiness. *Geophysical Research Letters*, 42(23).

Stocker, T., Qin, D., Plattner, G.-K., Alexander, L., Allen, S., Bindoff, N., Breon, F.-M., Church, J., Cubasch, U., Emori, S., Forster, P., Friedlingstein, P., Gillett, N., Gregory, J., Hartmann, D., Jansen, E., Kirtman, B., Knutti, R., Krishna Kumar, K., Lemke, P., Marotzke, J., Masson-Delmotte, V., Meehl, G., Mokhov, I., Piao, S., Ramaswamy, V., Randall, D., Rhein, M., Rojas, M., Sabine, C., Shindell, D., Talley, L., Vaughan, D., and Xie, S.-P. (2013). Technical summary. *Climate Change 2013: The Physical Science Basis. Contribution of Working Group I to the Fifth Assessment Report of the Intergovernmental Panel on Climate Change*, pages 33–115.

Stricevic, R., Cosic, M., Djurovic, N., Pejic, B., and Maksimovic, L. (2011). Assessment of the fao aquacrop model in the simulation of rainfed and supplementally irrigated maize, sugar beet and sunflower. *Agricultural water management*, 98(10):1615–1621.

Sutanudjaja, E., Van Beek, L., De Jong, S., Van Geer, F., and Bierkens, M. (2011). Large-scale groundwater modeling using global datasets: a test case for the rhine-meuse basin. *Hydrology and Earth System Sciences*, 15(9):2913–2935.

Sutanudjaja, E., Van Beek, L., De Jong, S., Van Geer, F., and Bierkens, M. (2014). Calibrating a large-extent high-resolution coupled groundwater-land surface model using soil moisture and discharge data. *Water Resources Research*, 50(1):687–705.

Tahri, K. (2012). Desalination in morocco: Challenges and prospects. In *International Conference on Desalination and Sustainability*.

Taky, A. (1996). Besoins en eau de la betterave a sucre et conduite de son irrigation selon le referentiel journalier de penman-monteith dans le perimetre du tadla. Insitut Agronomique et Vétérinaire Hassan II.

Todini, E. (1996). The arno rainfallrunoff model. *Journal of Hydrology*, 175(1):339–382.

Touchan, R., Anchukaitis, K. J., Meko, D. M., Attalah, S., Baisan, C., and Aloui, A. (2008). Long term context for recent drought in northwestern africa. *Geophysical Research Letters*, 35(13).

Van Beek, L. and Bierkens, M. F. (2009). *The global hydrological model PCR-GLOBWB: conceptualization, parameterization and verification.* Utrecht University, Utrecht, The Netherlands.

Van Beek, L., Wada, Y., and Bierkens, M. F. (2011). Global monthly water stress: 1. water balance and water availability. *Water Resources Research*, 47(7).

Van Lanen, H., Wanders, N., Tallaksen, L., and Van Loon, A. (2013). Hydrological drought across the world: impact of climate and physical catchment structure. *Hydrology and Earth System Sciences*, 17:1715–1732.

Vörösmarty, C., Fekete, B., Meybeck, M., and Lammers, R. (2000a). Global system of rivers: Its role in organizing continental land mass and defining land-to-ocean linkages. *Global Biogeochemical Cycles*, 14(2):599–621.

Vörösmarty, C. J., Green, P., Salisbury, J., and Lammers, R. B. (2000b). Global water resources: vulnerability from climate change and population growth. *Science*, 289(5477):284–288.

Wada, Y., van Beek, L., Viviroli, D., Dürr, H. H., Weingartner, R., and Bierkens, M. F. (2011). Global monthly water stress: 2. water demand and severity of water stress. *Water Resources Research*, 47(7).

Wada, Y., Wisser, D., and Bierkens, M. (2014). Global modeling of withdrawal, allocation and consumptive use of surface water and groundwater resources. *Earth System Dynamics*, 5(1):15.

Weedon, G. P., Balsamo, G., Bellouin, N., Gomes, S., Best, M. J., and Viterbo, P. (2014). The wfdei meteorological forcing data set: Watch forcing data methodology applied to era-interim reanalysis data. *Water Resources Research*, 50(9):7505–7514.

Wells, N., Goddard, S., and Hayes, M. J. (2004). A self-calibrating palmer drought severity index. *Journal of Climate*, 17(12):2335–2351.

Wilby, R. L. and Wigley, T. (2000). Precipitation predictors for downscaling: observed and general circulation model relationships. *International Journal of Climatology*, 20(6):641–661.

World Bank (2016). Project appraisal document on a proposed loan to the kingdom of morocco for a large scale irrigation modernization project. Technical report.

World Water Assessment Programme of the United Nations (2015). The united nations world water development report 2015: Water for a sustainable world. Technical report, UNESCO.

Zerouali, A. (2009). Institutional framework and decision making practices for water management in the oum er rbia basin, morocco. Technical report, ISKANE Ingeniére.

Zhou, T., Haddeland, I., Nijssen, B., and Lettenmaier, D. P. (2015). Human induced changes in the global water cycle. *AGU Geophysical Monograph Series*, Submitted.

Appendix A

Drought propagation, indicators and indices

The climatic change in Morocco is superimposed on a strong interannual variability, meaning that also without long term change an anomalous period of sustained droughts can occur. The high interannual variability is linked to the North Atlantic Oscillation (NAO), an atmospheric mode signified by the pressure difference between the Icelandic-low and the Azores-high. The mode influences flow according to its degree of expression (Cook et al., 2016; Milewski et al., 2015). In its negative phase, the pressure difference is smaller than normal, which forces the wintertime storm track to lie zonal, supplying moisture to the Mediterranean and Northern-Africa. While in the positive mode, the storm track shifts to north-western Europe, leading to below average atmospheric moisture in region. In winter and early spring, which are the dominant seasons of precipitation, the influence of this variable accumulation of moisture is particularly high (Driouech et al., 2009).

When an anomalous low amount of precipitation (a deficit relative to the normal) falls over a certain period one can speak of a *meteorological drought*. Due to the lowered precipitation, sometimes in combination with higher evaporation (in the form of temperature, radiation, wind or relative humidity perturbations (Allen et al., 1998)), the soil moisture close to the surface depletes. This direct influence on soil moisture conditions, often used for indicating drought (Wells et al., 2004; Schrier et al., 2013), is captured by the anomaly α in the average moisture storage of the first and second soil reservoir $S_1 + S_2$ (0-30 cm, figure 3.2) for a certain month m:

$$\alpha_m = S^m_{2,avg} - \overline{S^m_{2,avg}} \tag{A.1}$$

Where the 'normal' soil moisture condition $\overline{S^i_{2,avg}}$ is calculated over the time period 1979-2012.

After occurrence and propagation of an anomaly into the rootzones,

plants can evaporate less, and the lack of moisture recycling enhances the precipitation anomaly (Mohamed et al., 2005). The hinder of crop growth and terrestrial ecosystems is termed *agricultural drought* (Dai, 2011) and is indicated with the Aridity Anomaly Index AAI, the drop of actual evapotranspiration below its potential:

$$AAI = \frac{ET_{pot} - ET_{act}}{ET_{pot}} \cdot 100 \tag{A.2}$$

Which is also calculated at a monthly timescale.

With time, the subsurface flows equilibrate to the depleted soil moisture. Percolation lessens and capillary rise may enlarge, which, depending on the groundwater reservoir response characteristics, leads to reduced baseflow and surface water availability. This type of *hydrological drought* is evaluated through the behavior of Q_{80} (Van Lanen et al., 2013), the discharge threshold that is not exceeded in 20 percent of the time:

$$\Pr[Q_{tot} \leq Q_{80}] = \int_{-\infty}^{Q_{80}} f_Q(Q_{tot}) dQ = 0.2 \tag{A.3}$$

The pronounced multiyear component in Moroccan droughts has to do with the NAO's tendency to occur in decadal phases (El Jihad, 2003; Cook et al., 2016). But the prolonged memory in the system is also caused by vegetation feedbacks (Dai, 2011). When a drought for example leads to collapse of the ecosystem and degradation of an area, there will be less retention and percolation. Which lowers the water resources steadily provided by baseflow even in the years after the drought and prior to recovery.

The flows accumulate in the reservoirs of the basin. And as the volumes of water stored in reservoirs R_s are crucial for many users, resource scarcity becomes one of the socio-economic dimensions of droughts. In this study, isolated water availability A_{tadla} is formed by the summed reservoir storages supplying to the irrigated perimeter :

$$A_{tadla} = \sum_{i=1}^{n_{reservoirs}} R_{s,i} \tag{A.4}$$

The availability of a whole basin is often expressed per capita. Common thresholds are 1000 m^3/ca/yr for chronic water scarcity and 500 m^3/ca/yr for extreme water scarcity (Kummu et al., 2010; Arnell and Lloyd-Hughes, 2014). Currently, the Oum er Rbia basin experiences chronic water shortage (chapter 2).

Although useful for first indication, the availability does not tell whether the use of, and competition for, resources is high (Brauman et al., 2016). Therefore, availability is specifically related to usage in a Water Scarcity Index WSI. But the ways to quantify usage are numerous: from gross

water abstractions, to consumptive water use (the part of the withdrawn water that evapotranspires during use) and to net water abstractions (water abstractions minus return flows) (Döll et al., 2016). In this study gross abstraction (withdrawal) W is used for the index:

$$WSI = \frac{W}{A} \tag{A.5}$$

Kiguchi et al. (2015) define high water stress as a WSI above 0.4. And Falkenmark et al. (2007) mark economically damaging water scarcity as a WSI above 0.8. In this region however, with seasonal flow regimes, only computing the annual value may not grasp the stress experienced in summer. To reveal temporary stressful periods the index is therefore computed at monthly resolution (Wada et al., 2011; Brauman et al., 2016; Mekonnen and Hoekstra, 2016).

Additionally, impacts can be temporarily high but are also more impactful on vegetation and the stress experienced by humans when they recur often. This is quantified with the Dynamic Water Stress Index $DWSI$ that makes use of the monthly computed WSI values (Porporato et al., 2001; Wada et al., 2011). It accounts for the average stress in a period of prolonged stress, the frequency of prolonged stress and the resilience of the system:

$$DWSI = \left(\frac{\overline{\xi_s T_s}}{kT} \right)^{\frac{1}{\sqrt{f_s}}} \tag{A.6}$$

For a considered growing period of $T = 12$ months, the mean length of a prolonged stress period $\overline{T_s}$ is computed from all the months that WSI exceeds the 'high stress' threshold of 0.4. $\overline{\xi_s}$ is the average WSI for those periods of exceedence, which is counteracted by a dimensionless resilience k of 0.4 (Wada et al., 2011). f_s is the frequency that a stress period occurs in a growing period, calculated over the complete time period.

Appendix B

PCR-GLOBWB

The distributed model PCR-GLOBWB is forced by daily values of temperature, precipitation and reference evapotranspiration. It represents the hydrological processes on the surface, in multiple soil layers and in a groundwater store, on a cell-by-cell basis (Van Beek and Bierkens, 2009; Van Beek et al., 2011; Sutanudjaja et al., 2011, 2014; Wada et al., 2014). This makes it differ from STREAM (Balaghi et al., 2016) and purely conceptual models tested in a neighboring Moroccan catchment (Boulet et al., 2008).

For Oum Er Rbia, PCR-GLOBWB is set up with 3 soil layers (0-5 cm, 5-30 cm and 30-150 cm) and 1 groundwater reservoir (see figure 3.2). It runs at a spatial resolution of 0.08°x0.08° (approximately 10 km at the equator) and at a daily temporal resolution. The multiple stores can exchange water by percolation and capillary rise. The upper store can overflow at a certain threshold (though this threshold does not have to on-off but can be gradual (Hagemann and Gates, 2003)).

The precipitation P either falls as snow or as rain. In case of the former it is handled by a snow module, in case of the latter it first meets an interception store. This store has a maximum capacity Si_{max} that encompasses both canopy I_v and non-vegetative storage I_{nv} (e.g. puddles on rocks and roads):

$$Si_{max} = (1 - Cf) \cdot I_{nv} + Cf \cdot I_v \cdot LAI \tag{B.1}$$

Where the leaf area index LAI and the vegetated fraction of the cell Cf are monthly values. Both enlarge throughout the growing season from their minimum to their maximum values:

$$Cf_m = Cf_{min} + f_m \cdot (Cf_{max} - Cf_{min}) \tag{B.2}$$

$$LAI_m = LAI_{min} + f_m \cdot (LAI_{max} - LAI_{min}) \tag{B.3}$$

This progression is driven by f_m $[0, 1]$, an index for the deviation of monthly

temperature above the minimum temperature required for plant growth:

$$f_m = 1 - [(T_{max} - T_m)/(T_{max} - T_{min})]^2 \tag{B.4}$$

The minimum and maximum values of LAI are after Hagemann (2002) and accompany the GLCC 2.0 landcover product. This landcover product is aggregated to form the two vegetation classes of PCR-GLOBWB: short and tall vegetation (respectively: 'grass' and 'forest'), and additionally determines the vegetated fraction of a cell.

The input into the first soil store is the sum of non-intercepted- and excess-snow-meltwater (which was first stored in pore space of the snow). It can infiltrate wherever the soil is not saturated, the rest is partitioned as saturation overland flow (this is assumed to be the dominant direct runoff mechanism (Todini, 1996)). Variability in soil saturation within a gridcell is accounted for by the improved Arno-scheme (Hagemann and Gates, 2003):

$$s/S = 1 - [(W_{max} - W_{act})/(W_{max} - W_{min})]^b \tag{B.5}$$

s/S is the saturated fraction. W_{max} and W_{min} are storage capacities that represent the soil type variability within the gridcell, whereas W_{act} is the actual storage in the first and second layer. b is a shape parameter that describes the distribution of soil water storage in the cell. In steep terrain, the lower parts will for instance saturate quickly while in flat terrain the same amount of water does not surface anywhere (Hagemann and Gates, 2003). b is therefore based on the GLCC 2.0 maximum rooting depths and on elevation. A benefit of having a W_{min} is that this scheme does not generate runoff in very small rain events, while the original Arno scheme did (Todini, 1996). The model can however not include other direct runoff mechanisms such as overland flow by a surfacing groundwater table, because of the separation into stacked layers.

Downward fluxes between the layers $P_{i \text{ to } i+1}$ are equal to the unsaturated hydraulic conductivity k of the overlying layer i:

$$P_{i \text{ to } i+1}(t) = k_i(s_i(t)) \quad \text{for } i = 1, 2 \tag{B.6}$$

Unsaturated conductivity is a function of the average degree of saturation s_i in the gridcell. It is formed by the Campbell (1974) model fitted against the tabulated retention curves and unsaturated conductivity values for all soil types present in the gridcell:

$$k(s) = k_s s^{2\beta+3} \tag{B.7}$$

Where β is the Clapp and Hornberger (1978) constant in their relation for

the soil water retention curve:

$$\psi(s) = \psi_s s^{-\beta} \tag{B.8}$$

The upward fluxes from $P_{i+1 \text{ to } i}$ are zero when $s_i > s_{i+1}$. Otherwise they are driven by the soil moisture deficit of the overlying layer and are dependent on the unsaturated conductivity of the underlying layer:

$$P_{i+1 \text{ to } i} = k_{i+1}(s_{i+1}) \cdot (1 - s_i) \quad \text{for } i = 1, 2 \tag{B.9}$$

The percolation towards the groundwater reservoir S_4 is described by formula (9) in Van Beek and Bierkens (2009) and is constructed such that storage in the third soil reservoir S_3 cannot rise above field capacity. The same goes for capillary rise, but here also the groundwater table has to be within 5 m distance. The fraction of a cell with a groundwater table close enough to the surface is calculated from a highly detailed perennial stream network: for each of the high resolution cells the upstream catchment area is calculated including their groundwater height H:

$$H = \frac{W_4}{\text{specific yield}} = \frac{W_4}{\theta_s - \theta_r} \tag{B.10}$$

This height is added to the nearby stream level height (known from the routing procedure) to arrive at the groundwater table height.

Reference evapotranspiration ET_{ref} forms an important input. The evaporative demand is first met by water from the interception reservoir. This is modeled as open-water evaporation, using the crop-factor approach of Allen et al. (1998) to scale the reference evapotranspiration. Secondly the evaporation is met by water stored in the snowpack, modeled as bare soil evaporation, before it is passed on to transpiration and the real bare soil evaporation.

Bare soil evaporation is taken from the first soil store and is also approximated with a crop factor $k_{c,bare}$:

$$ET_{pot,bare} = k_{c,bare} ET_{ref} \tag{B.11}$$

In the saturated part of the gridcell enough water is available and the potential rate $ET_{pot,bare}$ is not reduced (although it cannot exceed the saturated hydraulic conductivity). In the unsaturated part the actual evaporation is a lowered form of the potential as it is reduced by saturation through the unsaturated hydraulic conductivity.

Transpiration through plants only takes place in the unsaturated fraction of the cells, because submerged roots prohibit it. In the unsaturated fraction of the cell $(1-x)$, a halving function prescribes limitation by average degree of saturation, including the fitted parameter from Clapp and Hornberger

(1978):

$$T = (1 - x) \cdot 1/(1 + (Se/Se_{50})^{-3 \cdot \beta}) \cdot T_{pot,crop} \tag{B.12}$$

Where $T_{pot,crop}$ is the crop specific potential evaporation after evaporation from interception. Se_{50} describes the soil saturation at a matric suction of 33.3 kPa and is a weighted composition of up to three soil layers with root presence, which is also the case for the composite actual saturation Se. Additionally, each month that LAI changes, the crop factors for the short and tall vegetation change with it. They vary between kc_{min} and kc_{max} (taken from Hagemann (2002)), as proposed by Allen et al. (1998).

Baseflow is assumed to be linearly related to the amount of water in the groundwater store. Parameterization of the reservoir coefficient follows the approach of Kraijenhoff Van De Leur (1958). Interflow is accounted for, as it can play a role in mountainous areas with regolith close to the surface. This approach is based on Sloan and Moore (1984) in which the soil is idealized as a uniform inclined slab with average depth. When the three outflows from a certain cell are summed (Direct runoff + Interflow + Baseflow) they form the locally generated runoff that proceeds to routing. Routing is performed in daily steps along the river network based on the Simulated Topological Networks (STN30) (Vörösmarty et al., 2000a).

To summarize one of the sophisticated features of PCR-GLOBWB: Subgrid variability incorporates information on the fractional coverage: short and tall vegetation and open water. Regarding the improved ARNO scheme it includes: different soil types, vegetation types and elevation differences. For transpiration it includes the different vegetation types and soil types.

The snow module of PCR-GLOBWB is based on the HBV-degree-day snow model by Bergström (1976), meaning that the snowmelt is only temperature driven. When temperatures are below zero degree Celcius all prescribed precipitation falls as snow. It accumulates into the snowpack and melts proportional to the temperature rise above a threshold T_{th}. In its extensive formulation previous melt and ripening of the snowpack are accounted for by enlarging the melt factor (C_0) accordingly:

$$Melt = C_0 \cdot (1 + C_{eff} \sum Melt) \cdot (T - T_{th}) \tag{B.13}$$

Open waterbodies form a separate landcover class and are modeled with a balance: direct inputs are formed by precipitation and lateral inflow, and direct outputs by open water evaporation, discharge and water consumption. The water height of all surface water bodies (lakes and reservoirs) is treated as variable while their extent is fixed, but further treatment differs per type. Lakes are seen as stores that will overflow through a rectangular cross section above a certain threshold, as prescribed by the weir formula of Bos et al. (1989). For the reservoirs a prognostic operation scheme is used: A current release decision is based on future projections (next months inflow

and demand) from past average values (Van Beek et al., 2011).

The demand module employs 0.08°x0.08° maps, where (i) livestock is the product of livestock density and the consumptive use per unit, (ii) industrial demand consists of water for energy production and manufacturing and (iii) domestic water demand is modeled as a variable dependent on: population, GDP and technological progress[1]. For irrigation, the map does not signify demand but only the location of irrigated area. It is created by pattern scaling the timeseries of countrywide total area with the current spatial distribution.

The original dynamic irrigation water requirement calculation (that can be switched off) treats paddy and non-paddy crops separately (Wada et al., 2014). The paddies are simulated with a 5 cm water layer that is maintained until the near-harvest stage in the cropping calendar. Calendars and the associated growing stages are obtained from the MIRCA2000 dataset (Portmann et al., 2010), and the corresponding crop coefficients from Siebert and Döll (2010). The presence of a multiple crops is handled by a weighted aggregation of the factors to a single fictional crop (Wada et al., 2014). Each daily step, a water balance for the 5 cm layer (including open water evaporation) is evaluated, which makes the water requirement equal to the amount of percolation and evaporation, minus precipitation. For the non-paddy type, the irrigation water requirement is modeled as a deficit in soil water availability. According to Allen et al. (1998) the Total Available Water is the difference between water content at field capacity and at wilting point, over the length of the rooting zone:

$$TAW[mm] = (\theta_{fieldcap} - \theta_{wilting}) \cdot \text{rooting depth}[mm] \tag{B.14}$$

In PCR-GLOBWB this maximum amount of water available to plants is expressed similarly, though distributed over the discrete soil layers. The actual Readily Available Water (RAW) in the profile is a similar difference, but then between current content and content at wilting point. The amount of water applied by irrigation is equal to the deficit ($TAW - RAW$). This however, is only applied when the RAW drops below the practically extractable total amount of water $p(t) \cdot TAW$. Where:

$$p(t) = p_{ref} + 40 \cdot (0.005 - T_c) \tag{B.15}$$

This empirical relation expresses the fact that a crop transpiration T_c that exceeds the rate of transportation to the roots will also result in water stress.

[1]The approach of translating gridded population densities to the domestic water demand per cell is justified because population growth has been a main driver of water withdrawal (Kummu et al., 2010). Technological development or economic growth can be used to add a temporal component to published statistics (Flörke et al., 2013).

Appendix C

AquaCrop

Before the existence of AquaCrop it was empirically known that long term crop yield (relative to its potential) was related to the actual evapotranspiration from an area (also relative to the potential) (Doorenbos and Kassam, 1979). As research progressed, the multiple relations underlying this finding became quantifyable and meaningful at timescales of days (Steduto et al., 2009, 2012; García-Vila and Fereres, 2012). This enabled the improvement of yield assessments and got formalized in the model AquaCrop (Raes et al., 2012). It is forced by daily values of precipitation, minimum and maximum air temperature and reference evapotranspiration ET_{ref}.

On the daily timescales the attainment of crop biomass B is related to the amount of transpired water T_a:

$$B = WP \cdot \sum \frac{T_a}{ET_{ref}} \tag{C.1}$$

Where WP is the normalized (relative to the FAO reference crop) water productivity in [kg biomass m^{-2} mm transpiration^{-1}]. The main benefit of this approach is that WP is conservative for a given nutrient level, almost regardless of water stress. Biomass (which is seen as disconnected from root development and canopy growth) is converted into the harvestable portion, yield Y, via a harvest index HI:

$$Y = HI \cdot B \tag{C.2}$$

Depending on the crop, and the phenological stage it is in, this translation can be lagged. A cereal for example only starts grain development after a certain stage of growth. The main factors influencing the crop's dynamics are temperature and soil water content. A comprehensive overview is provided by figure C.1.

The temperature values can be reworked to Growing Degree Days, that provide a drive for the different developmental stages: flowering, root/tuber

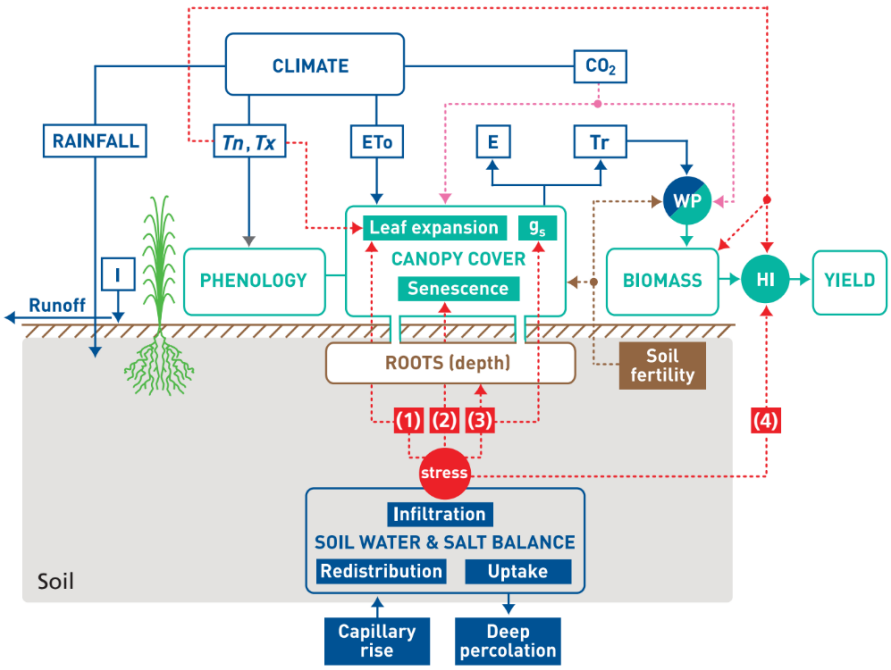

Figure C.1: AquaCrop flowchart of the soil-plant-atmosphere continuum (Steduto et al., 2012)

initiation, time of maximum rooting depth, start of canopy senescence and physiological maturity (Steduto et al., 2012). In this case however, they are driven by time in days. Temperature also influences WP, as it can be too cold for growth, and HI, as it can be too hot or cold for pollination.

Soil water content is calculated as a balance and available water comes in through precipitation and irrigation, where rainfall is partitioned into runoff and infiltration according the Curve Number approach. The water content can exert stress on WP and HI, but these are relatively stable. The more dynamic responses to water stress occur via three feedbacks: (i) reduction of canopy expansion rate, (ii) closure of stomata (lowering stomatal conductance g_s) and (iii) acceleration of senescence.

Looking at the stage of canopy development (before senescence), the model uniquely does not take Leaf Area Index but Canopy Cover CC as variable. It is a composite of multiple plants:

$$CC = \text{plant density [plant} \quad m^{-2}] \cdot \text{cover per plant } [m^2 \quad \text{plant}^{-1}] \quad \text{(C.3)}$$

and has a canopy growth coefficient CGC that is influenced by water stress:

$$CC = CC_0 \exp(CGC \cdot t) \quad \text{(C.4)}$$

$$CC = CC_{max} - (CC_{max} - CC_0) \exp(-CGC \cdot t) \quad \text{(C.5)}$$

These two are relations exemplary of the many parameterized relations that describe natural development in the model. In the senescence stage, CC is for example differently expressed and differently influenced by water stress. Because of the different responses, the coefficients including the starting CC_0 and maximum values CC_max are subject to calibration. Root deepening is modeled with a minimum effective rooting depth and a maximum effective rooting depth (which is reached near end of growing). At every quarter of the effective rooting depth respectively 40, 30, 20 and 10 percent is taken up (when available).

Within the soil part of the continuum, the 1D model simulates flow through a finite difference approach on 12 soil compartments, at a daily timestep. An outgoing flux of percolation is considered, but the incoming capillary rise is not, because the groundwater table of Tadla is at 20+ m depth (Kselik et al., 2008; Hennebert and Moerenhout, 2007). The hydraulic characteristics that the model uses include: a drainage coefficient τ, hydraulic conductivity k_{sat} and volumetric water contents θ_{sat}, θ_{fc}, θ_{wp} (see also table 3.1). The water that is theoretically available is the difference between the content θ at field capacity and that at wilting point, integrated over the rooting depth. The deviation from what is theoretically available is called rootzone depletion p. And when it surpasses a certain threshold, this rootzone depletion translates to the water stress coefficient K_s with shape parameter f:

$$K_s = 1 - \frac{e^{p \cdot f} - 1}{e^f - 1} \tag{C.6}$$

The K_s is directly applied as a limitation of potential transpiration, see equation (C.7), while the effects of water stress on the stomatal conductance, canopy growth coefficient and root deepening are described through intermediate relations, see Raes et al. (2012, ch.3).

If there is no limitation of stomatal opening, then transpiration is almost linear to the canopy coverage. The slight deviation is caused by a micro oasis-effect (interrow advection of energy) that adds to the energy available for transpiration by radiation balance only. When the stomatal limitation k_{sto} and the crop coefficient k_c are included, the relationship for actual transpiration T_a becomes:

$$T_a = k_{sto} \cdot k_c \cdot K_s \cdot CC \cdot ET_{ref} \tag{C.7}$$

Because of the inter row advection of energy, the unshaded bare soil is assumed to be a little less than $(1 - CC)$. For a fully wet soil surface the bare soil evaporation is a little more than ET_{ref}, while during drying it declines exponentially with the wetness in the uppermost soil layer.

Appendix D

Computations behind the Methodology

The interaction between water use and the available resources is present in all river basins with human regulation. Most basically this interaction is formed by a withdrawal that lowers the current and near-future resources at that location, and possibly at other (downstream) locations too[1] (Döll et al., 2014). In PCR-GLOBWB this 'update' of the resources is made for each daily time step, but in Approaches 1 and 2 the isolated availability needs to be updated afterwards to get an actual availability.

For these two approaches, it was established in the methodology that the extracted reservoir storage is not a full accumulation of all water. It is isolated in the sense of 'none is yet extracted for agriculture' but it is also subject to reservoir overflow rules. This means that it should not be updated with all withdrawals up to a certain time step. It requires us to account only for the withdrawals within a moving window. This window has an assumed size of twelve months because (i) operators have planned their releases such that after a full operational year they approximate the same target storage and (ii) the superimposed circumstances of high or low recharge are already in the isolated storage.

Approach 1 combines the extensive requirements for good yield with the actual availability to indicate water stress. According the moving window, actual storage A_i is the result of the requirements W of the previous twelve months from the isolated availability B_i. Which makes the water stress for month i equal to:

$$WSI_i = \frac{W_i}{A_i} = \frac{W_i}{B_i - \sum_{j=1}^{12} W_{i-j}} \tag{D.1}$$

[1]The lowering of availability at other times and locations feels intuitive for surface waters, but occurs in groundwater too: either via the water budget (Bredehoeft, 2002) or via reduced baseflow (Wada et al., 2014).

Table D.1: Measured groundwater contributions of (Kwelde, 2006). And relative importance based on Chahri and Saouabe (2014, table 16), Akdim (2014, table 28) and Kwelde (2006, table 23). No groundwater contribution was measured for maize so assumed to be zero. Cotton assumed as important as maize.

	Alfalfa	Wheat	Maize	Sugar beet	Citrus	Olive	Cotton
Contribution g_c [-]	0.5	0.3	0	0.39			
Importance f_{imp} [-]	24872	4730	9459	12251	13598	9240	9459

Where the extensive surface water requirements [m^3] are the result of an upscaling procedure of AquaCrop's intensive requirements iwr [mm] for the four crops c:

$$W_i = 10 \cdot \sum_{c=1}^{4} iwr_c \cdot P_c \cdot \frac{1}{s} \cdot ((1 - f_{gw}) + f_{gw}(1 - g_c)) \tag{D.2}$$

Where the ten is a unit conversion, $s = 0.8$ is the surface water distribution efficiency (Zerouali, 2009), P_c is the areal abundance of the crop according the cropping pattern of the respective year. And where g_c is the groundwater contribution measured at farms using groundwater (table D.1). But this latter correction only needs to be applied to the fraction of farms with access to the groundwater resource $f_{gw} = 0.47$ (Kuper et al., 2012).

Approach 2 translates the impacts on surface water availability to impacts on yield, meaning that the total irrigation application iwr is now an input to AquaCrop, and is computed with the moving window for actual storage and a downscaling procedure. Operational practice is captured with releases that are a fixed proportion f_{rel} (for correspondence to the historical statistics assumed 10 percent) of the actual storage. A release R for month i becomes:

$$R_i = f_{rel} \cdot A_i = f_{rel} \cdot \left(B_i - \sum_{j=1}^{12} W_{i-j} \right) \tag{D.3}$$

This release is divided over all 7 dominant crops (table D.1), to make sure that realistic amounts are found for the 4 modeled ones. A division key is constructed from on-field measurements of the amounts of water applied per crop. These relative importances f_{imp} can be seen as a parametric approach to the common division of water, given equal presence on the field (table D.1). But because the areas of the crops are far from equal, the area of a certain crop is 'distorted' by its importance and divided by the distorted

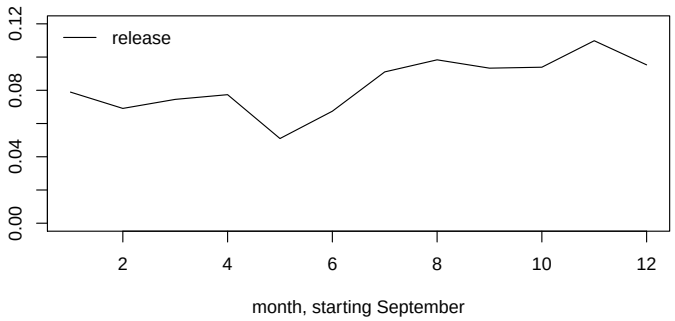

Figure D.1: Projection of annual values for an agricultural campaign based on release statistics 2012-2016 supplied by ORMVAT.

total:

$$\frac{A_{dis,c}}{A_{dis,tot}} = \frac{f_{imp,c} \cdot P_c}{\sum_{k=1}^{7} f_{imp,k} \cdot P_k} \tag{D.4}$$

Which is used to arrive at the intensive total amounts per crop, including the contribution of groundwater, distribution efficiency and unit conversion:

$$iwr_c = R_i \cdot s \cdot \frac{1}{10} \cdot \frac{A_{dis,c}}{A_{dis,tot}} \cdot \frac{1}{P_c} \cdot \frac{1}{(1 - f_{gw}) + f_{gw}(1 - g_c)} \tag{D.5}$$

For Approach 3 the AquaCrop withdrawals per agricultural season needed to be supplied as monthly input to PCR-GLOBWB. Therefore a multiplication vector was constructed from daily release data for the years 2012-2016 supplied by ORMVAT. The releases were summed for the months and normalized to form the factors that upon multiplication with an annual value give the corresponding monthly one. From figure D.1 can be seen that it has a seasonal pattern of higher summer demands. The same key was used to construct the monthly statistics in the left panel of figure 4.9.